KLK3/PSA and cathepsin D activate VEGF-C and VEGF-D

Sawan Kumar Jha[1,2*]; Khushbu Rauniyar[1*]; Ewa Chronowska[1,3]; Kenny Mattonet[4]; Eunice Wairimu Maina[1]; Hannu Koistinen[5,6]; Ulf-Håkan Stenman[5,6]; Kari Alitalo[2,6,7]; Michael Jeltsch[1,2**]

[1]Individualized Drug Therapy Research Program, University of Helsinki, Finland; [2]Wihuri Research Institute, Helsinki, Finland; [3]Jagiellonian University Medical College, Cracow, Poland; [4]Max Planck Institute for Heart and Lung Research, Bad Nauheim, Germany; [5]Department of Clinical Chemistry, University of Helsinki, Finland; [6]Helsinki University Hospital, Helsinki, Finland; [7]Translational Cancer Medicine Research Program, University of Helsinki, Finland

*These authors contributed equally to the research.

**Author for correspondence: Dr. Michael Jeltsch, Individualized Drug Therapy Research Program and Wihuri Research Institute, Biomedicum Helsinki, P.O.B. 63 (Haartmaninkatu 8), 00014 University of Helsinki, Finland; Phone: +358-2941-25514; Fax: +358-2941-25510; E-mail: michael@jeltsch.org

ABSTRACT

Vascular endothelial growth factor-C (VEGF-C) acts primarily on endothelial cells, but also on non-vascular targets, e.g. in the CNS and immune system. Here we describe a novel, unique VEGF-

C form in the human reproductive system produced via cleavage by kallikrein-related peptidase 3 (KLK3), aka prostate-specific antigen (PSA). KLK3 activated VEGF-C specifically and efficiently through cleavage at a novel N-terminal site. We detected VEGF-C in seminal plasma, and sperm liquefaction occurred concurrently with VEGF-C activation, which was enhanced by collagen and calcium binding EGF domains 1 (CCBE1). After plasmin and ADAMTS3, KLK3 is the third protease shown to activate VEGF-C. Since differently activated VEGF-Cs are characterized by successively shorter N-terminal helices, we created an even shorter hypothetical form, which showed preferential binding to VEGFR-3. Using mass spectrometric analysis of the isolated VEGF-C-cleaving activity from human saliva, we identified cathepsin D as a protease that can activate VEGF-C as well as VEGF-D.

Key Words: kallikrein-related peptidases, lymphangiogenesis, KLK3, PSA, cathepsin D, VEGF-C, VEGF-D

INTRODUCTION

Vascular endothelial growth factor VEGF-A is essential for early embryonic development and for successful implantation of the embryo into the uterus (Binder et al., 2014). VEGF-A acts in this function on both vascular and non-vascular targets (Hannan et al., 2011). The primary function of the closely related growth factor VEGF-C is stimulation of growth of the lymphatic vasculature (Rauniyar et al., 2018). It is required for ovarian follicle growth and maturation and endometrial lymphangiogenesis (Rogers, 2008; Rutkowski et al., 2013). Unlike VEGF-A, which is secreted as an active growth factor (Leung et al., 1989), VEGF-C is secreted as an inactive precursor (pro-VEGF-C), which requires two proteolytic cleavages for activation (Jeltsch et al., 2014; Joukov et al., 1997). The first C-terminal cleavage resulting in pro-VEGF-C occurs constitutively in the endoplasmic reticulum and is mediated by protein convertases (Siegfried et al., 2003). The second cleavage step takes place in the extracellular environment, is highly regulated and requires the assembly of a trimeric complex consisting of VEGF-C, the ADAMTS3 metalloproteinase and the "cofactor" CCBE1 (Bui et al., 2016; Jeltsch et al., 2014). Alternative activation by plasmin has been shown in vitro, but its significance under physiological settings is unknown (McColl et al., 2003). VEGF-D is the closest paralog of VEGF-C (Achen et al., 1998). Similar to VEGF-C, it is lymphangiogenic (Veikkola et al., 2001), but appears to have a higher angiogenic potential than VEGF-C (Byzova et al., 2002; Rissanen et al., 2003). The proteolytic activation of VEGF-D is very similar to that of VEGF-C (Stacker et al., 1999a), but it deploys distinct, so far unknown proteases (Bui et al., 2016).

Many kallikrein-related peptidases are highly expressed in the prostate, and some prostate-derived cell lines, such as the immortalized human normal prostate epithelial (NPrEC) or PC-3 cells — from which VEGF-C was originally cloned — express high amounts of VEGF-C (Grennan, 2006; Joukov et al., 1996). In a peptide library scan, Matsumura et al. identified VEGF-C as a potential

substrate for KLK4 (Matsumura et al., 2005). Based on these observations, we tested human kallikrein-related peptidases for their ability to activate VEGF-C. In this study, we show that KLK3, the major protease in human semen, is able to specifically activate VEGF-C and VEGF-D. We further show that cathepsin D cleavage of VEGF-C results in a novel, predominantly VEGFR-3-binding form of VEGF-C, and that cathepsin D cleavage of VEGF-D at the homologous site results in a VEGFR-2-specific (minor mature) form of VEGF-D.

RESULTS

VEGF-C is processed by the kallikrein-related peptidase 3 (KLK3)

While we could not demonstrate robust VEGF-C activation by KLK4 as predicted by Matsumura (Matsumura et al., 2005) (data not shown), purified KLK3 cleaved pro-VEGF-C, resulting in a mature protein that migrated at about 20 kDa in Western blotting analysis (Figure **1A**, lane 2). To confirm that KLK3 was responsible for the cleavage, we inhibited its protease activity by using the monoclonal antibody 5C7 (Stenman et al., 1999) in 2-fold molar excess (Figure **1A**, lane 1 versus lane 2). We probed the polypeptide bands resulting from the cleavage with rabbit antiserum 6 and antiserum 3/4, which were raised against full-length and mature VEGF-C, respectively (Figure **1A and B**, compare the second lanes). Probing with antiserum 3/4, which recognizes both pro-VEGF-C and mature VEGF-C, showed that the majority of pro-VEGF-C had been cleaved by KLK3.

KLK3-processed VEGF-C is biologically active

We tested the KLK3-processed VEGF-C for its biological activity in Ba/F3 cells, which had been stably transfected with VEGFR/EpoR chimeras and found that it promoted the survival of both VEGFR-2/EpoR (Figure **1C**) and VEGFR-3/EpoR cells (Figure **1D**).

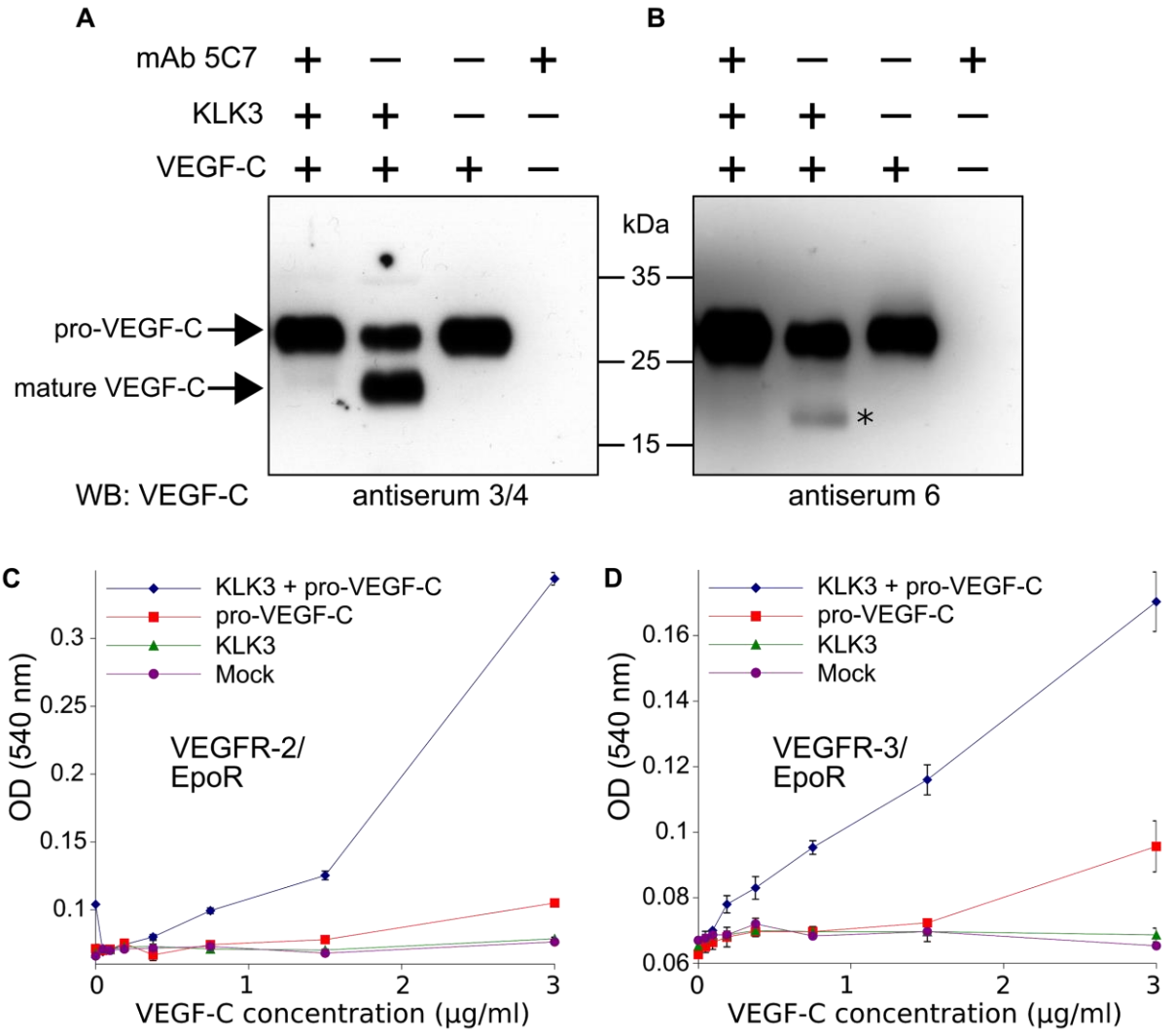

Figure 1. Kallikrein-related peptidase 3 (KLK3) / Prostate-specific antigen (PSA) activates VEGF-C. (A, B) Cleavage of pro-VEGF-C by KLK3 (PSA). Pro-VEGF-C was incubated with or without KLK3, with and without the monoclonal antibody against KLK3 (5C7). Detection of VEGF-C in Western blots probed with antiserum 6 and 3/4, resulting in the detection of pro-VEGF-C (29/31 kDa) and activated, mature VEGF-C (21/23 kDa). The band marked by the asterisk likely represents the N-terminal propeptide (~15 kDa) which is detected by the antiserum 6. Note that for the image shown for antiserum 6, two different exposures of the same blot were merged (n=3). (C, D) VEGF-C processed by KLK3 is biologically active in Ba/F3 cell assays, which translate

activation of a hybrid VEGFR/EpoR receptor into cell survival (n=2). Error bars indicate SD.

KLK3 activation of VEGF-C results in a unique VEGF-C species

Edman degradation of the KLK3-processed species of VEGF-C revealed the amino-terminal sequence NTEIL (Figure 2-figure supplement 1 and 2). Thus, KLK3 cleaves VEGF-C between Tyr-114 and Asn-115, targeting a sequence similar to most of its cleavage sites in the seminogelins, which are the primary target proteins of KLK3 (Malm et al., 2000). The KLK3-cleaved VEGF-C is three N-terminal amino acid residues shorter than the mature VEGF-C generated by ADAMTS3 (Jeltsch et al., 2014) and 12 amino acid residues shorter than the mature VEGF-C produced by PC-3 cells (Figure **2**) (Joukov et al., 1997). We analyzed the VEGF-C amino acid sequences of 40 vertebrate species and found that residues -7 to +1 relative to the KLK3 cleavage site and -4 to +4 relative to the ADAMTS3 cleavage site (KFAA↓AHY↓N) are 100% conserved among all mammals and birds that were included in the analysis. However, we found significant differences in this area in all fish species analyzed (Figure 2-figure supplement 3).

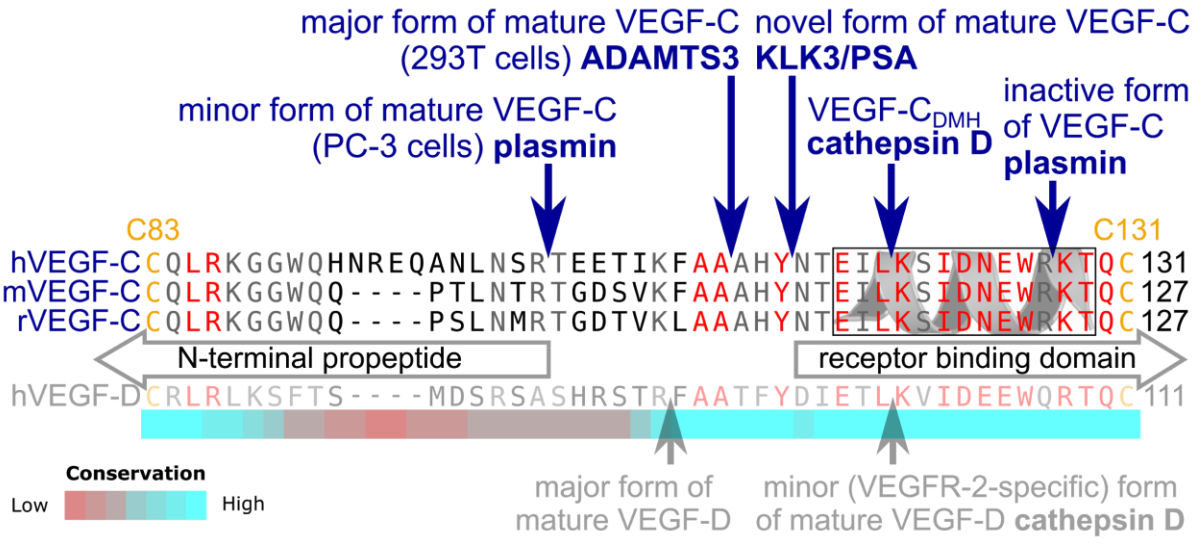

Figure 2. KLK3 activation of VEGF-C results in a unique VEGF-C species. KLK3 cleavage results in a mature VEGF-C species that is N-terminally three amino acids shorter than the ADAMTS3-cleaved VEGF-C. Shown are the aligned amino acid sequences between the N-terminal propeptide and the receptor binding domain of VEGF-C in human (h), mouse (m) and rat (r)VEGF-C and hVEGF-D. The arrows mark the sites of proteolytic cleavage of all four reported VEGF-C-activating enzymes and the two reported cleavage sites in VEGF-D. Residues within the N-terminal alpha-helix of VEGF-C/D are boxed. Note that the 1st plasmin cleavage site was not verified experimentally, but deduced from the plasmin cleavage signature and the size of the resulting product. The heat map under the alignment indicates the areas of highest divergence, deduced from a more comprehensive alignment of VEGF-C orthologs (see Figure 2-figure supplement 3).

Human seminal fluid contains VEGF-C

To evaluate the biological significance of VEGF-C activation by KLK3, we first analyzed the VEGF-C content of human seminal plasma. Because of difficulties in detecting VEGF-C at low ng/ml-range concentrations in a high-protein sample (~50 mg/ml) like semen (Owen, 2005), we first compared the ability of different anti-VEGF-C antibodies to detect VEGF-C (Figure 3-figure supplement 1, Supplementary File 1). VEGF-C was detected in Western blots of sperm liquefied for approximately 20-30 min at room temperature by using antibody sc-374628 after VEGF-C precipitation with soluble forms of its receptors VEGFR-2 (VEGFR-2/Fc) and VEGFR-3 (VEGFR-3/Fc) or anti-VEGF-C antiserum 882 (Figure **3A**). The affinity of seminal plasma VEGF-C towards VEGFR-2 appeared to be much weaker than towards VEGFR-3 in the VEGF-C pull down assay (Figure **3A**, compare lanes 4 and 6). The mobilities of the VEGF-C polypeptides indicated that it is composed of inactive pro-VEGF-C and active mature VEGF-C. Stimulation of VEGFR-3-

transfected porcine aortic endothelial (PAE) cells with seminal plasma resulted in VEGFR-3 phosphorylation (Figure **3B**, compare lanes 2 and 4). VEGF-C stimulation of PAE cells stably expressing VEGFR-2 led to an even stronger phosphorylation than the recombinant VEGF-C control. We reasoned that this could indicate the presence of VEGF-A, whose concentrations in seminal plasma have been reported to range from less than 2 ng/ml to more than 100 ng/ml in seminal plasma (Obermair et al., 1999). Indeed, most of the VEGFR-2 phosphorylation was blocked when incubated with soluble VEGFR-2/Fc, but not by incubation with VEGFR-3/Fc (Figure 3-figure supplement 2). In contrast, VEGF-D was not detected in seminal plasma (Figure 3-figure supplement 3).

VEGF-C is activated during sperm liquefaction

When fresh ejaculates were immediately mixed with protease inhibitors, placed on ice and analyzed, less active VEGF-C was detected than in ejaculates that had been liquefied, indicating that pro-VEGF-C is converted into mature VEGF-C after ejaculation (Figure **3C**)**,** concurrently with sperm liquefaction. Lowering the pH with citric acid tended to increase slightly the yield of mature VEGF-C (Figure **3C**, lane 5), but ion chelation with CHELEX 100 or EDTA had no effect (Figure **3C**, lanes 2 and 4, respectively).

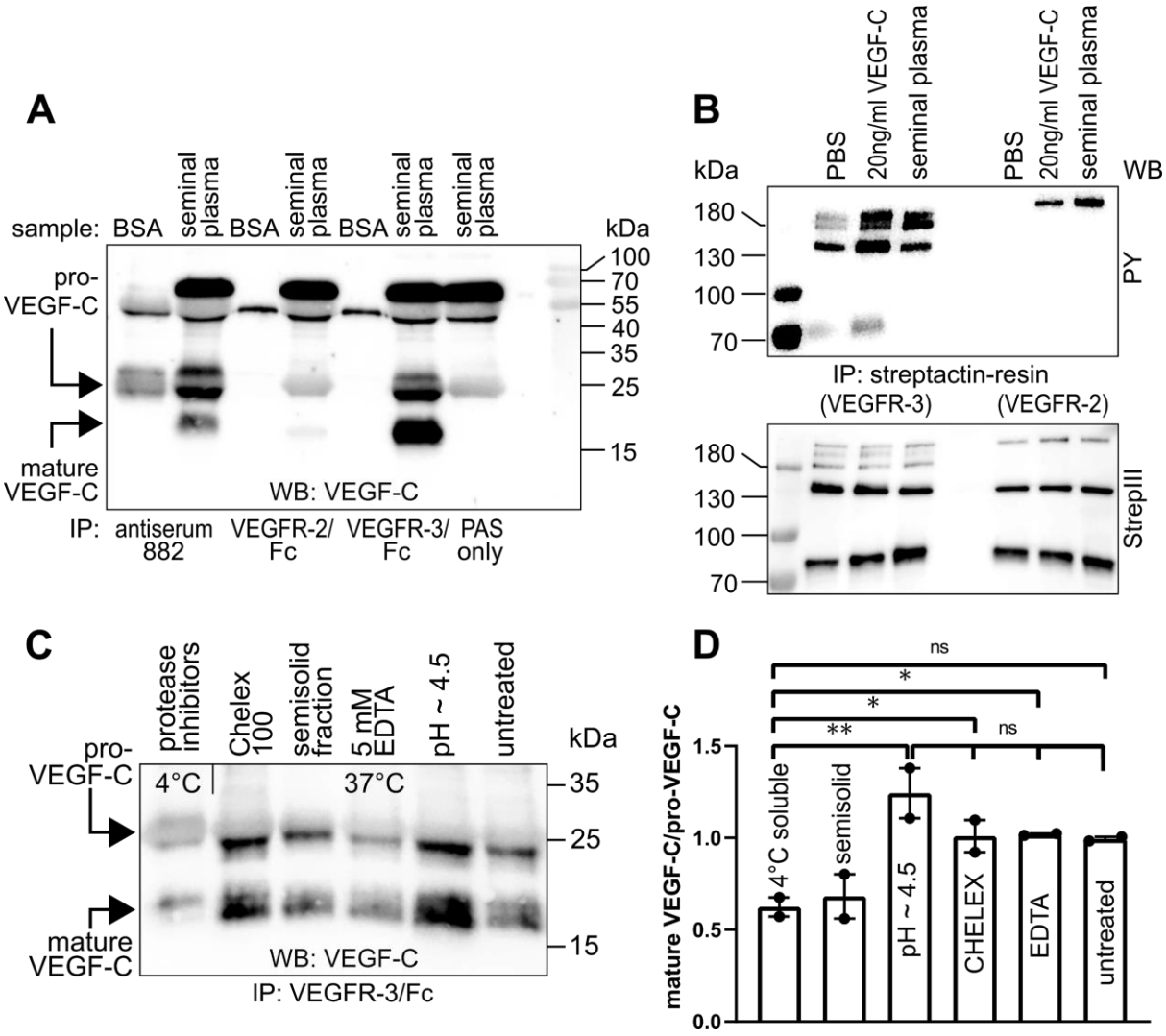

Figure 3. Seminal plasma VEGF-C is cleaved during sperm liquefaction and binds and activates VEGFR-3. (A) Detection of both pro-VEGF-C and activated, mature VEGF-C by Western blotting with anti-VEGF-C antibody sc-374628 after pull-down with soluble VEGF receptors or antiserum 882. (B) Phosphorylation of VEGFR-2 and VEGFR-3 by seminal VEGF-C. Note that the phosphorylation pattern of VEGFR-3 is slightly different from that induced by 20 ng/ml of the VEGF-C control protein, which corresponds to the plasmin-activated form of VEGF-C. The lower panel shows the same blot reprobed with Streptactin-HRP for detection of the total levels of VEGFR-3 and VEGFR-2, respectively. (PAS, protein A sepharose; PY, phosphotyrosine) (C) Fresh seminal fluid contains less processed VEGF-C than seminal fluid liquefied at 37°C,

indicating that pro-VEGF-C is converted into mature VEGF-C after ejaculation. Effect of protease inhibitors and low temperature on cleavage of VEGF-C (lane 1). While the mature VEGF-C/pro-VEGF-C ratios of ion sequestered samples (50 mg/ml CHELEX 100 and 5 mM EDTA in lanes 2 and 4, respectively) were not different from the untreated sample (lane 6), lowering the pH tended to increase the activation of VEGF-C (lane 5), but the difference to untreated sample did not reach statistical significance. Note that non-liquefied and liquefied samples differ because the semisolid seminogelins largely disappear during liquefaction (Malm et al., 2000). The semisolid fraction of fresh ejaculate was separately assessed for its VEGF-C content after liquefaction (lane 3). (D) Quantification of the ratio of mature VEGF-C to pro-VEGF-C in seminal plasma exposed to different conditions. Comparison of the 4°C sample to pH~4.5 ($p=0.0066$), CHELEX ($p=0.045$), untreated ($p=0.052$), and EDTA ($p=0.042$) [One-way ANOVA, Dunnett's multiple comparisons test ($n=2$), data are presented as mean±SEM].

VEGF-C processing by KLK3 is enhanced by CCBE1

We have shown that CCBE1 enhances the proteolytic activation of VEGF-C by ADAMTS3, but not by plasmin (Jeltsch et al., 2014). Therefore, we tested whether CCBE1 would accelerate KLK3 activation of VEGF-C. We found that KLK3-mediated cleavage of VEGF-C was enhanced by CCBE1 when CCBE1 or KLK3 amounts were titrated down so that only little VEGF-C processing occurred (Figure **4**). Substantial amounts of CCBE1 were detected in seminal plasma by Western blotting (Figure 4-figure supplement 1), confirming published proteomics results (Jodar et al., 2015). This indicates that VEGF-C cleavage could be increased by CCBE1 also in semen.

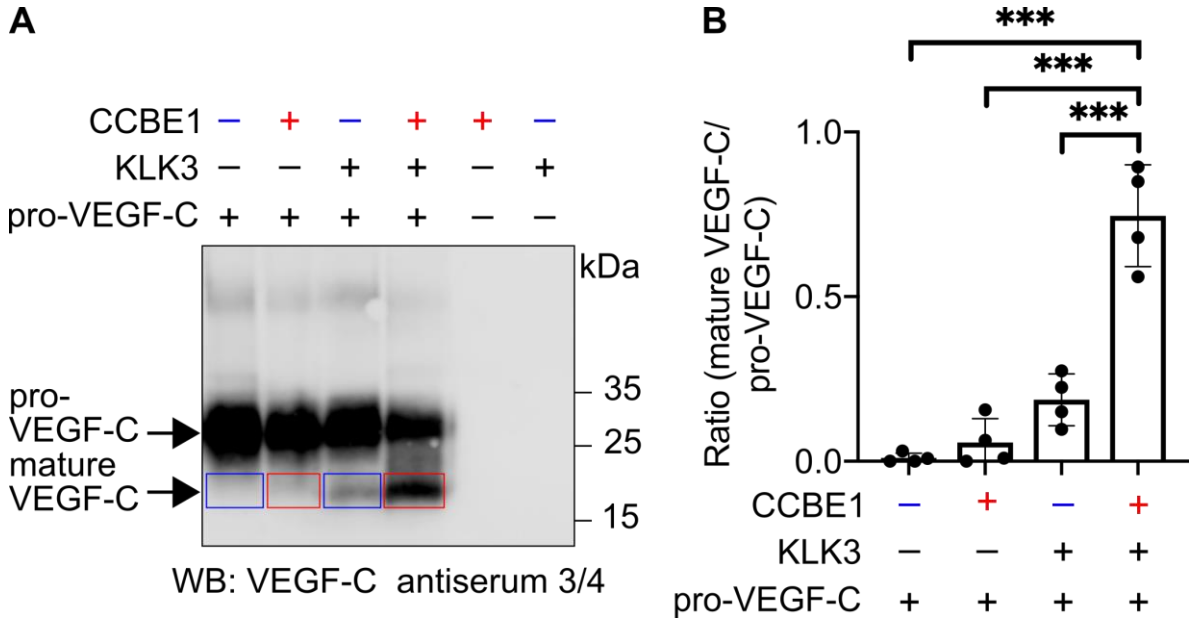

Figure 4. VEGF-C activation by KLK3 is enhanced by CCBE1. (A) Activation of VEGF-C by KLK3 is enhanced by CCBE1. The mature VEGF-C produced in the presence or absence of CCBE1 is shown in the red and blue boxes, respectively. (B) Quantification of the mature VEGF-C/pro-VEGF-C ratio. Data are shown as mean ± SD (n=4). Statistical differences were determined by one-way ANOVA with Tukey *post hoc* test, ***P<0.001.

VEGF-C and VEGF-D activities have different sensitivities to N-terminal truncations

Activated VEGF-C binds to VEGFR-2 (Joukov et al., 1997), but in our assays with seminal plasma, VEGFR-2 binding was very weak (Figure **3A**, lane 4). To explain this finding, we focused on the cleavage of the N-terminal helix, because its partial removal in VEGF-D decreases selectively VEGFR-3 binding while leaving VEGFR-2 binding intact (Leppanen et al., 2011). Since complete proteolytic removal of the N-terminal helix of VEGF-C abolishes all receptor binding and phosphorylation-stimulating activity (Jeltsch et al., 2014), we first tested if a partial removal of the

N-terminal helix (cutting between Leu-118 and Lys-119, corresponding to the proteolytic cleavage site between Leu-114 and Lys-115 of VEGF-D) would result in a selective loss of VEGF-C binding to its receptors.

The protease that cleaves between Leu-114 and Lys-115 of VEGF-D (and hypothetically between the homologous Leu-118 and Lys-119 of VEGF-C) is unknown. Therefore, we generated this form of VEGF-C by truncating the VEGF-C cDNA, which was then expressed in S2 cells. Interestingly, unlike the corresponding VEGF-D form, this "VEGF-C_{DMH}" (for "D Minor Homology") bound to VEGFR-3, but only weakly or not at all to VEGFR-2 (Figure **5A**). Because of this unexpected result, we performed the experiment using proteins produced in 293T cells and found that in conditions where all other mature forms of VEGF-C interacted with their receptors as predicted, VEGF-C_{DMH} did not bind to VEGFR-2 or VEGFR-3 (Figure **5B**). Since the loss of binding compared to the S2 cell-produced VEGF-C_{DMH} is not associated with a loss of receptor-interacting amino acid residues, we attributed the loss of binding to the extra N-terminal four amino acid residues of the mammalian linker (see also Figure 5-figure supplement 1).

We then used equimolar amounts of truncated VEGF-Cs expressed in transiently transfected CHO cells (Figure 5-figure supplement 1**)** to test the bioactivity of different N-terminally truncated VEGF-Cs in VEGFR-2 and VEGFR-3 phosphorylation assays. The receptor phosphorylation results mirrored the binding results. The longest mature VEGF-C resulted in the strongest stimulation, and progressive shortening of the N-terminus resulted in gradually decreased stimulation of the receptor phosphorylation (Figure **5C**). We also tested the activity of purified VEGF-C_{DMH} expressed in S2 cells. In agreement with the binding results, 100ng/ml VEGF-C_{DMH} did stimulate the phosphorylation of VEGFR-3 but not or only very weakly of VEGFR-2 (Figure **5D**).

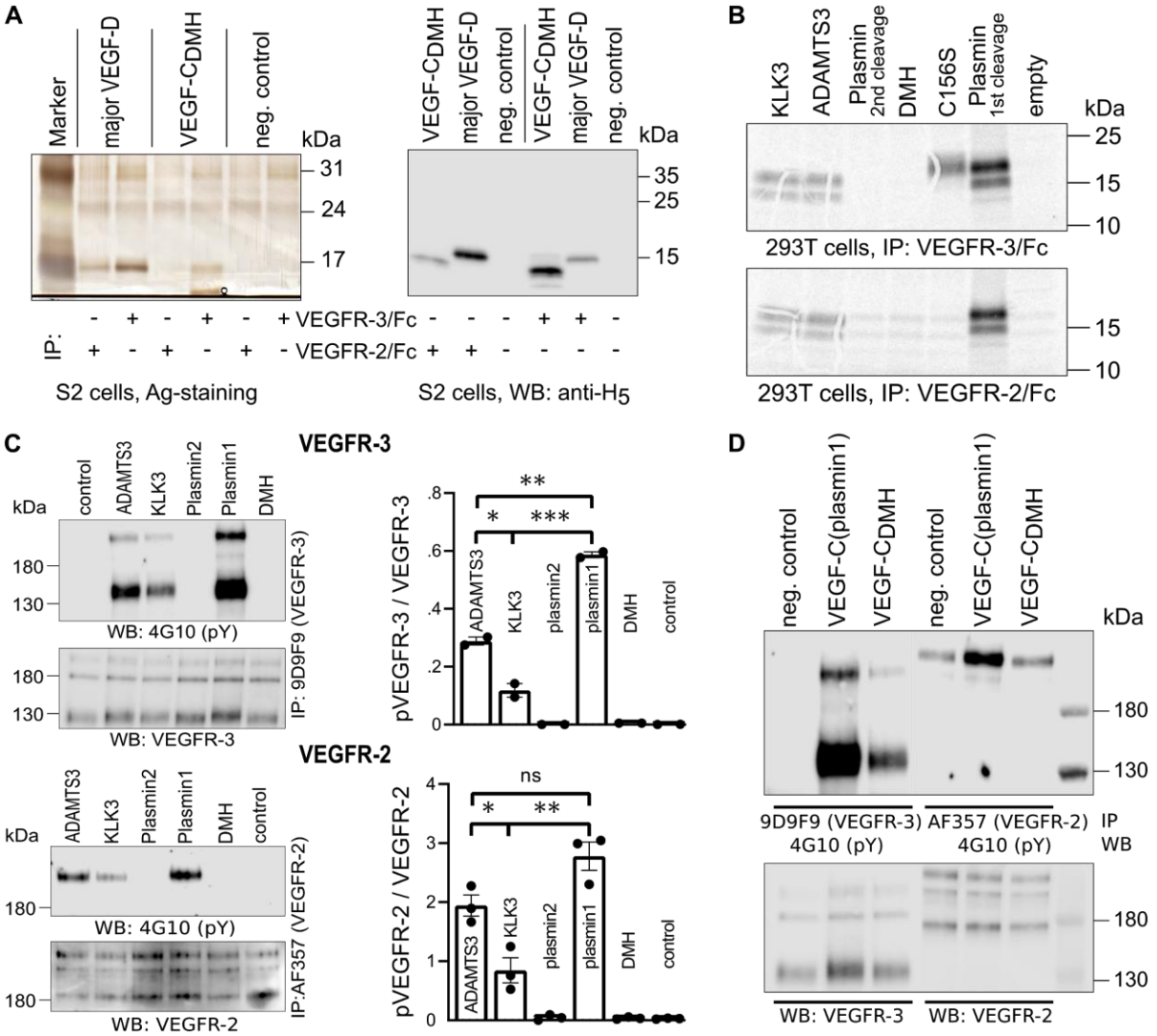

Figure 5. Shortening of the VEGF-C N-terminal helix reduces receptor binding and activation. (A) VEGF-C_{DMH} form binds efficiently to VEGFR-3 but weakly to VEGFR-2 when expressed in S2 cells. (B) Lack of binding of 293T-produced VEGF-C_{DMH} to VEGFR-2 or VEGFR-3. Note that the weak bands visible in the mock transfected 293T samples are due to endogenous VEGF-A, which binds to VEGFR-2, but not to VEGFR-3 (n=2). (C) Stimulation of VEGFR-3 and VEGFR-2 phosphorylation by equimolar amounts of N-terminally truncated VEGF-Cs (corresponding to mature VEGF-C generated by ADAMTS3, KLK3, and the first plasmin cleavage) expressed in CHO cells (quantification: n=2 for VEGFR-3; n=3 for VEGFR-2; data are presented as

mean±SEM; one-way ANOVA, Tukey's multiple comparisons test). When compared with control, all three mature VEGF-C forms show significant stimulation of both receptors (p-values = 0.0094 to <0.0001). (D) Phosphorylation of hVEGFR-3 but not hVEGFR-2 in PAE cells by VEGF-C_{DMH} purified from S2 cells.

A comparison of the sizes of VEGF-C polypeptides produced by S2 cells transfected with N-terminally truncated cDNAs encoding the polypeptide resulting from cleavage by ADAMTS3 and the (longer) form generated by the 1st plasmin cleavage revealed bands of identical size, indicating additional proteolytic processing (Figure 5-figure supplement 1). N-terminal sequencing of the form produced from the longer cDNA revealed that about ⅔ had the KSIDNE… N-terminus, and about ⅓ had AAAHYN... as N-terminus. Hence, the DMH-form of mature VEGF-C can also be produced by proteolytic processing of a longer mature form of VEGF-C by a yet unknown protease. We refer to such cleavage on top of an existing activation in the following as *secondary activation* (irrespectively of the receptor activation ability of the resulting protein species).

Cathepsin D activates both VEGF-C and VEGF-D

The presence of a VEGF-C-cleaving protease in seminal fluid prompted us to search for such a protease also in other body fluids. We enriched the VEGF-C activating component of human saliva by cation exchange chromatography (Figure 6-figure supplement 1) and subjected the fractions containing the peak activity to mass spectrometric analysis. Among the highest scoring proteases (Supplementary File 2), cathepsin D was identified as the most likely candidate due to the cleavage context of the DMH-form of VEGF-C (Leu-118↓Lys-119). Using purified recombinant proteins, we confirmed that cathepsin D cleaves pro-VEGF-C into active VEGF-C (Figures **6A** and **7AB**) and

performs a *secondary activation* of the minor, mature form of VEGF-C (Figure **7F**). Because the sequence contexts of the cleavage sites of cathepsin D and KLK3 are conserved between VEGF-C and VEGF-D (see Figure **2**), we investigated, if also cathepsin D and KLK3 could activate pro-VEGF-D. Indeed, cathepsin D activates pro-VEGF-D and performs a *secondary activation* of the longer, mature form of VEGF-D. The cleavage of mature VEGF-D was rapid and complete (Figure **6C**), whereas the cleavage of both pro-VEGF-C and mature VEGF-C was slower and incomplete even after 16 hours (Figure **6AB**). As expected, the cathepsin D processing of mature VEGF-D abolished most of its activity in the Ba/F3-VEGFR-3/EpoR assay (Figure **7C**) and reduced, but did not abolish its activity in the Ba/F3-VEGFR-2/EpoR assay (Figure **7D**), while processing of pro-VEGF-D stimulated the phosphorylation of VEGFR-2 (Figure 7-figure supplement 1). KLK3 also activated pro-VEGF-D (Figure **6D** and **7E**). When VEGF-D was produced from a full-length cDNA using the baculovirus system, a significant fraction of the protein did not undergo processing by protein convertases. This allowed us to observe two additional KLK3 cleavage sites in pro-VEGF-D. One of these cleavages has been reported previously (Stacker et al., 1999a); the other cleavage mimics the C-terminal cleavage catalyzed by protein convertases that cleave between the VHD and the N-terminal propeptide (Figure **6D** and Figure 7-figure supplement 2).

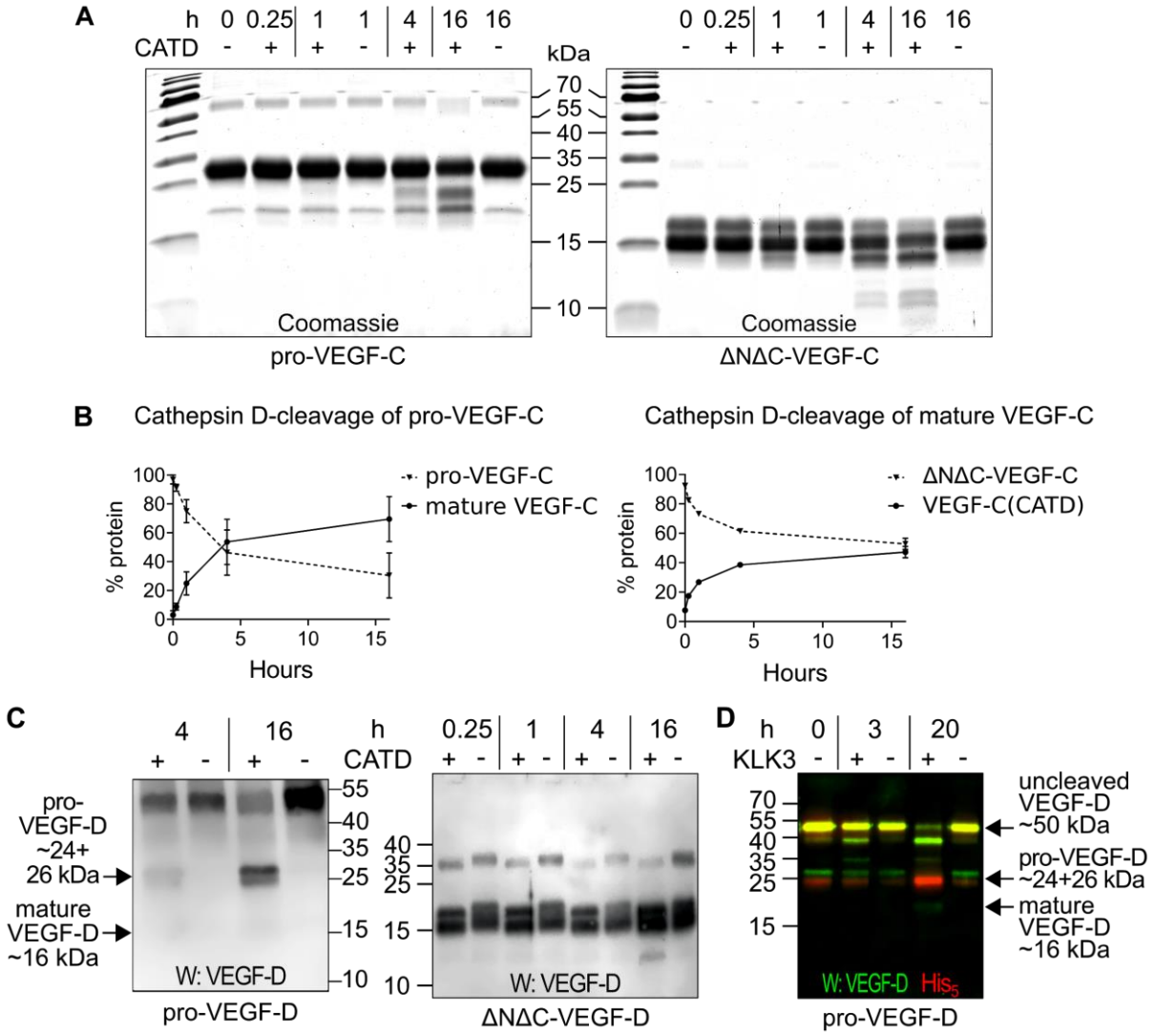

Figure 6. Cathepsin D activates pro-VEGF-C/D and mature VEGF-C/D, respectively. (A) Cleavage of VEGF-C by coincubation of pro-VEGF-C with cathepsin D (left panel) and secondary activation of ΔNΔC-VEGF-C (a mature form of VEGF-C translated from a truncated cDNA, right panel). (B) Quantification of the cleavage of pro-VEGF-C (n=3) and ΔNΔC-VEGF-C (n=2) by cathepsin D. (C) Cathepsin-D-mediated conversion of pro-VEGF-D into mature VEGF-D (left panel), and rapid activation of ΔNΔC-VEGF-D (a mature form of VEGF-D translated from a truncated cDNA, right panel). (D) pro-VEGF-D is cleaved by KLK3. Note that, KLK3 cleaves VEGF-D between the VEGF homology domain and the N-terminal propeptide, but also between the

269 VEGF homology domain and the C-terminal propeptide (for a detailed breakdown of the cleavage
270 products visible in this overlay and the individual exposures, see Figure 7-figure supplement 2)
271 (n=2).

272

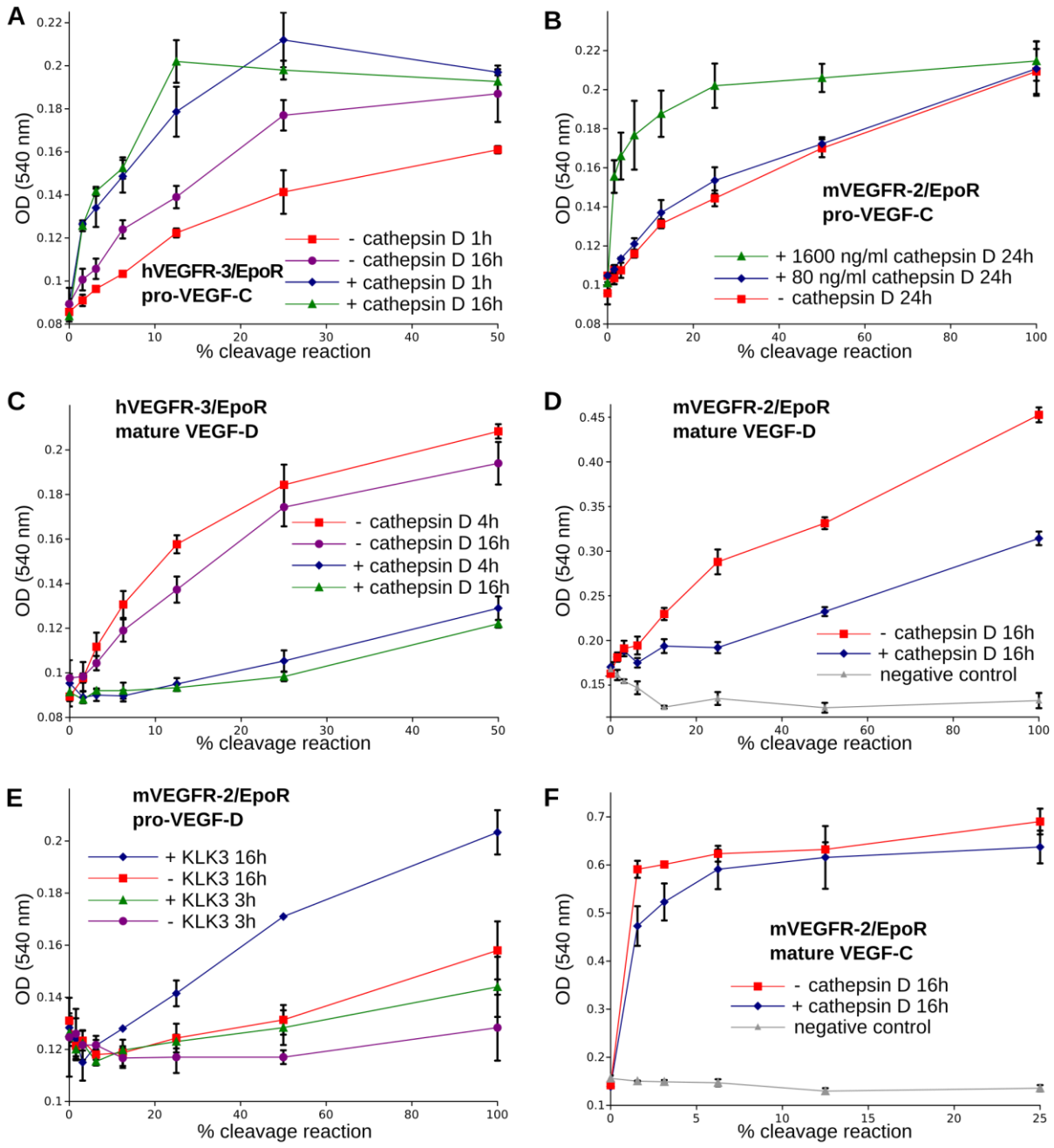

273

274 **Figure 7. The receptor-activating properties of VEGF-C and VEGF-D are differentially**

affected by cathepsin D cleavage. Shown are the results of Ba/F3-VEGFR/EpoR assays used to evaluate the receptor-activating properties of cathepsin D- and KLK3- cleaved proteins. Cathepsin D-cleaved VEGF-C activity in the (A) Ba/F3-VEGFR-3/EpoR assay and (B) Ba/F3-VEGFR-2/EpoR assay. (C) Mature VEGF-D after secondary activation with cathepsin D in the Ba/F3-VEGFR-3/EpoR assay. (D) The minor form of mature VEGF-D generated by cathepsin D-cleavage is less active than the major mature form in the Ba/F3-VEGFR-2/EpoR assay. (E) KLK3 activation of VEGF-D increases its potency in the Ba/F3-VEGFR-2/EpoR assay. (F) The secondary activation of mature VEGF-C with cathepsin D led to a small decrease in the response of Ba/F3-VEGFR-2/EpoR cells (n=2). Error bars indicate SD.

In vivo effects of the novel mature VEGF-C forms

To confirm that the two new forms of VEGF-C have also an effect in-vivo, we transduced skeletal muscle (tibialis anterior) of mice with recombinant adeno-associated viruses serotype 9 encoding the KLK3- or the cathepsin D- (CATD) form of VEGF-C. Both vectors stimulated lymphangiogenesis and angiogenesis. As expected on the basis of the binding and receptor phosphorylation results, the response to the KLK3-form was stronger compared to the cathepsin D-form. Both forms appeared to give a stronger response compared to the positive control (the ADAMTS3-form of VEGF-C), but the higher expression level of the shorter VEGF-C forms likely explains most of this difference (Figure 8-figure supplement 1).

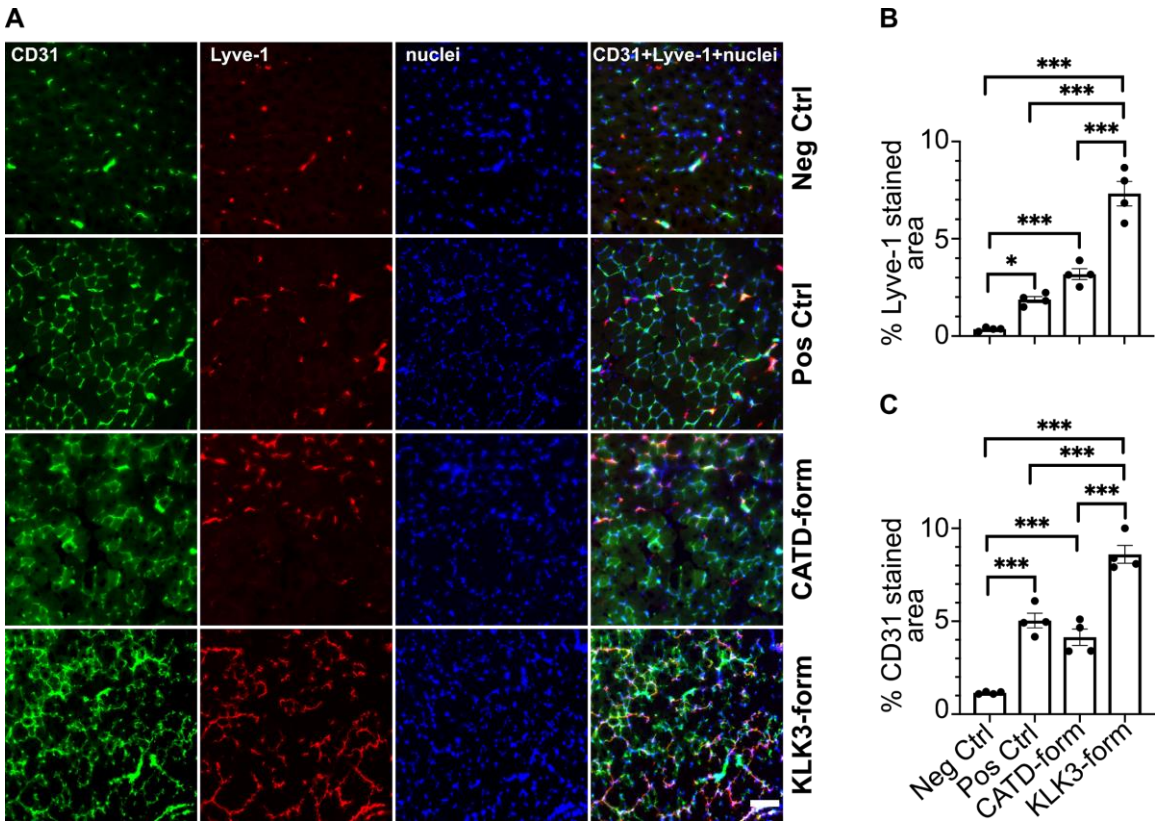

Figure 8. The KLK3- and cathepsin D-forms of VEGF-C induce lymphangiogenesis and angiogenesis in vivo. (A) Shown are the immunofluorescent stainings of the blood and lymphatic vessels in skeletal muscle transduced with recombinant adeno-associated virus subtype 9 (AAV9) encoding the KLK3- or the cathepsin D (CATD)-form of VEGF-C. Quantification of (B) Lyve-1 positive stained area and (C) CD31 positive stained area in AAV9 transduced tibialis anterior muscle. Data are presented as mean±SEM, n=4, one-way ANOVA with Tukey's *post hoc* test, ***P<0.001, *P<0.05. Scale bar, 100 µm. (see also Figure 8-figure supplement 1).

DISCUSSION

Kallikrein-related peptidase 3 (KLK3) or prostate-specific antigen (PSA) is widely known as a

prostate cancer marker (Lilja et al., 2008), which may also participate in prostate cancer development (Koistinen and Stenman, 2012). PSA/KLK3 is also the major protease responsible for seminal clot liquefaction, and thus plays a role in reproduction. In our study, we have found an unexpected link between these apparently separate functions in the form of Vascular Endothelial Growth Factor-C (VEGF-C) and VEGF-D.

Requirement for VEGFs during reproduction

The angiogenic effect of VEGF-A is required e.g. for implantation (Torry et al., 2007) and corpus luteum formation (Reynolds et al., 2000). VEGF-A levels in human seminal plasma are variable, typically between 10-20 ng/ml (Brown et al., 1995; Obermair et al., 1999), and VEGF-A has been implicated as a fertility factor acting on sperm cells (Obermair et al., 1999). Sperm motility has been reported to increase slightly as a response to VEGF-A (Iyibozkurt et al., 2009), and a testis-specific VEGF-A transgene overexpression resulted in infertility (Korpelainen et al., 1998). VEGF-C is the lymphangiogenic counterpart of VEGF-A, and lymphangiogenesis is required for ovarian follicle maturation (Rutkowski et al., 2013), corpus luteum formation (Abe et al., 2014; Nitta et al., 2011) and uterine implantation (Red-Horse, 2008). Furthermore, VEGF-C and VEGF-D are hormonally regulated in the reproductive system (Nitta et al., 2011).

KLK3/PSA as a VEGF-C activator

The prostate produces KLK3 and contributes active KLK3 to semen. KLK3 is the major protease in semen and participates in seminal clot liquefaction. KLK3 from human seminal plasma cleaved VEGF-C between its N-terminal propeptide and the VEGF homology domain. Compared to the major form of mature VEGF-C, the form produced by KLK3 lacks three amino acid residues from the N-terminus but it still activated both VEGFR-2 and VEGFR-3. In vitro, both sperm liquefaction

and VEGF-C exposure to KLK3 resulted in efficient cleavage of VEGF-C. However, in natural insemination, several factors, such as the vaginal environment or the absent mixing of the early prostatic fraction with the seminal vesicular fluid fraction (Björndahl and Kvist, 2003) may interfere with VEGF-C activation.

Apart from KLK3, seminal plasma also contains many other proteases involved in the proteolytic liquefaction cascade (Emami and Diamandis, 2013), which might contribute to VEGF-C activation (and inactivation), including cathepsin D (this study) and plasmin (Jeltsch et al., 2014; Stief, 2007). Similar to seminal plasma TGF-β (Robertson et al., 2002), which is also activated during liquefaction (Emami and Diamandis, 2010), VEGF-C might also contribute to the impregnation-associated immunomodulation. Several types of immune cells express VEGF-C receptors (Hamrah et al., 2003; Krebs et al., 2012; Li et al., 2016), and VEGF-C may be responsible for the immune tolerance of uterine NK cells during pregnancy (Kalkunte et al., 2009). However, since KLK3 exists only in higher primates (Pavlopoulou et al., 2010), any function of KLK3-mediated VEGF-C activation in seminal fluid is difficult to address experimentally. On the other hand, mice have many kallikrein-related peptidases that have no human counterparts (Pavlopoulou et al., 2010), and one of these might functionally replace KLK3 as an activator of VEGF-C. Unlike in mice, KLK3 prevents copulatory plug formation in humans, where sperm liquefaction is thought to be a physical requirement for sperm movement (Mann and Lutwak-Mann, 2012).

KLK3 and tumor (lymph)angiogenesis

VEGF-A inhibition marked a conceptual breakthrough in antiangiogenic cancer treatment (Ferrara et al., 2005). Although every single VEGF paralog in humans (PlGF, VEGF-B, VEGF-C, VEGF-D) has been proposed to mediate the tumor escape under anti-VEGF-A treatment (Li et al., 2014; Lieu et al., 2013), only VEGF-C and VEGF-D activate VEGFR-2 and VEGFR-3 (Achen et al., 1998;

Joukov et al., 1996) and are therefore prime suspects (Kubota, 2012; Li et al., 2014; Stacker et al., 2001; Wang and Tsai, 2015). VEGF-A is able to activate VEGFR-2 immediately after secretion, but VEGF-C and VEGF-D need to be proteolytically processed to become angiogenic (Joukov et al., 1997; Stacker et al., 1999a) or lymphangiogenic (Jeltsch et al., 2014).

The significance of KLK3/PSA for tumor progression is still debated with studies arguing both in favor or against a tumor-promoting function of KLK3 (Fortier et al., 1999; Ishii et al., 2004; LeBeau et al., 2010; Mattsson et al., 2008; Webber et al., 1995). KLK3 expression is largely restricted to the male prostate ("ist.medisapiens.com," 2019; Shaw and Diamandis, 2007), but small amounts can be found in other tissues, like the female homolog to the prostate, Skene's gland (Zaviacic and Ablin, 2000). In the pathological setting, the highest expression levels are found in prostate cancers ("ist.medisapiens.com," 2019). We have hypothesized that KLK3 may facilitate early development of prostate cancer, but at later stages slow down the cancer growth (Koistinen and Stenman, 2012). VEGF-C expression, which overlaps in the prostate with KLK3 expression (Joory et al., 2006), is similarly controversial with some studies supporting (Jennbacken et al., 2005; Yang et al., 2014) and others refuting (Mori et al., 2010) the predictive ability for prostate cancer progression. Most experimental animal models confirm the role of VEGF-C for metastatic spread (Brakenhielm et al., 2007; Burton et al., 2008), and potential mechanisms have been identified in cell culture models (Rinaldo et al., 2007). This study shows that, at least in principle, KLK3 could contribute to the activation of tumor-derived VEGF-C or VEGF-D and thus to a (lymph)angiogenic tumor phenotype.

How does CCBE1 accelerate VEGF-C activation?

KLK3 is a serine protease, but like ADAMTS3, its activity towards VEGF-C was increased by CCBE1. This reinforces the view that CCBE1 interacts with VEGF-C in the trimeric VEGF-

C/ADAMTS3/CCBE1 complex, removing the masking of the cleavage site by the C-terminal domain of VEGF-C (Joukov et al., 1997). This idea is supported by the ability of the isolated C-terminal domain of VEGF-C to competitively inhibit CCBE1-accelerated VEGF-C activation by ADAMTS3 (Jeltsch et al., 2014; Jha et al., 2017). It would also explain why VEGF-C activation by plasmin is not controlled by CCBE1, as the plasmin cleavage site is located ~10 amino acids residues further away from the receptor binding epitope than the ADAMTS3 and KLK3 cleavage sites (see Figure **2**).

Cathepsin D activates VEGF-C and VEGF-D with different outcomes

VEGF-C_{DMH} was a designed variant with an N-terminal cleavage resembling that in the minor (VEGFR-2-specific) form of VEGF-D. After we had established that VEGF-C_{DMH}-like form is produced by cathepsin D via proteolytic cleavage of a longer VEGF-C polypeptide, we confirmed that also the VEGFR-2-specific form of VEGF-D (minor, mature form) is indeed produced by cathepsin D cleavage. However, cathepsin D cleavage affects VEGF-C and VEGF-D differently. While VEGF-D loses practically all binding affinity towards VEGFR-3, VEGF-C seems to lose preferentially its affinity towards VEGFR-2.

The minor mature form of VEGF-D was identified in the supernatant of VEGF-D-producing 293 cells (Stacker et al., 1999a), where VEGF-C_{DMH} was not detected (Joukov et al., 1997), presumably because cathepsin D-cleavage of VEGF-C is inefficient. Alternatively, the ADAMTS3-cleavage of VEGF-C in 293 cells may have preemptively removed the recognition epitope required for cathepsin D cleavage.

Secondary cleavage results in additional VEGF-C and VEGF-D species

Our data show that the longest forms of mature VEGF-C and VEGF-D can undergo secondary

activation (i.e. N-terminally cleaved on top of a prior, activating cleavage). This introduces an additional layer of complexity into the regulation of VEGF-C and VEGF-D signaling since the cathepsin D-cleavage abolishes the VEGFR-3 binding of VEGF-D and reduces the VEGFR-2 binding of VEGF-C.

Cathepsin D is ubiquitously expressed, and although predominantly involved in lysosomal protein degradation (Benes et al., 2008), it can be secreted and soluble cathepsin D is found in saliva (our present findings) and in seminal plasma (Jodar et al., 2015). Secondary activation by cathepsin D may explain why we saw only weak VEGF-C-VEGFR-2 interaction when analyzing seminal plasma. It should be noted that cathepsin D has also been implicated in cancer metastasis (Benes et al., 2008; Spyratos et al., 1989), where VEGF-C has been shown to play a role (Karpanen et al., 2001; Mandriota et al., 2001; Skobe et al., 2001). However, the cathepsin D-mediated secondary activation of the major, mature form of VEGF-D was very rapid, when compared to the very slow activation of VEGF-C (compare Figures **6A** and **6C**). Therefore, VEGF-D activation appears to be the more relevant function of cathepsin D than VEGF-C activation. The cathepsin D-processed minor form of mature VEGF-D showed a lower potency to activate VEGFR-2 than the major form of mature VEGF-D, likely reflecting the corresponding K_D values (Leppanen et al., 2011). Despite this, as a net effect, cathepsin D cleavage of VEGF-D may result in increased angiogenic activity.

The role of the N-terminal helix

In VEGF-A, the N-terminal helix in the VEGF homology domain appears essential for the receptor dimerization and activity (Siemeister et al., 1998), whereas the platelet derived growth factor does not need an N-terminal helix for receptor binding (Muller et al., 1997; Shim et al., 2010). The Leu119↓Lys120 (cathepsin D) cleavage of VEGF-C happens within the N-terminal helix, which contains binding epitopes for VEGFR-2 (Leppänen et al., 2010). The N-terminal helix also interacts

with VEGFR-3. However, mutating the contacting amino acid residues Asp123 and Gln130 only ameliorates binding of VEGF-C to VEGFR-3 (Leppänen et al., 2013). The present receptor phosphorylation data strongly suggests that shortening of the helix leads to decreased activation of both VEGFR-2 and VEGFR-3, whereas a complete or near-complete removal of the N-terminal alpha helix- e.g. by extended plasmin exposure - abolishes all receptor binding. Inline with this, both the KLK3- and the cathepsin D-forms of VEGF-C induced lymphangiogenesis and angiogenesis in skeletal muscle. The N-terminal helix of VEGF-C is largely conserved among vertebrates, but C-terminal end of the N-terminal propeptide and linker preceding the VEGF homology domain represent the most diverse sequences among VEGF-Cs in different species. Between fish and the rest of the vertebrate clade, these differences are especially noticeable (Figure 2-figure supplement 3), indicating potential differences in the VEGF-C activation.

Separate activating proteases for each specific task?

Although ADAMTS3 appears to be responsible for developmental lymphangiogenesis only, our study indicates that other proteases may activate VEGF-C for specific niche functions, for example KLK3 in the reproductive system. The possible involvement of cathepsin D and KLK3 in tumor metastasis could be addressed in the appropriate gene-targeted mouse models. The possible other niche functions of VEGF-C, for example in the central nervous system (Mackenzie and Ruhrberg, 2012), in osmoregulation (Machnik et al., 2009) or in the immune system (Loffredo et al., 2014), may also be controlled by differentially regulated proteases.

MATERIALS AND METHODS

Key resources table

Reagent type (species) or resource	**Designation**	**Source or reference**	**Identifiers**	**Additional information**
cell line *(M. musculus)*	Ba/F3-hVEGFR-3/ EpoR	(Achen et al., 2000)		Murine pro-B cells expressing a chimeric VEGFR-3, from reference lab
cell line *(M. musculus)*	Ba/F3-mVEGFR-2/EpoR	(Stacker et al., 1999b)		Murine pro-B cells expressing a chimeric VEGFR-2, from reference lab
cell line *(Sus scrofa domesticus)*	PAE-VEGFR-3-StrepIII	(Leppänen et al., 2013)		Porcine aortic endothelial cells expressing strep-tagged VEGFR-3, from reference lab
cell line *(Sus scrofa domesticus)*	PAE-VEGFR-2-StrepIII	(Anisimov et al., 2013)		Porcine aortic endothelial cells expressing strep-tagged VEGFR-2, from reference lab
cell line *(Sus scrofa domesticus)*	PAE-VEGFR-3	(Pajusola et al., 1994)		Porcine aortic endothelial cells expressing untagged VEGFR-3, from reference lab
cell line *(Sus scrofa domesticus)*	PAE-VEGFR-2	(Waltenberger et al., 1994)		Porcine aortic endothelial cells expressing untagged VEGFR-2, from reference lab
cell line *(Homo sapiens)*	293T	ATCC	RRID:CVCL_0063	Human embryonic kidney cells, from vendor
cell line (*Cricetulus griseus)*	CHO DG44	Invitrogen		Chinese hamster ovary cells, from vendor
cell line *(Drosophila melanogaster)*	Schneider S2 cells	Invitrogen		Insect cells for protein production (*Drosophila* expression system), from vendor
cell line *(Spodoptera frugiperda)*	Sf9	Invitrogen		Insect cells for protein production (FactBac system), from vendor
transfected construct	pMT-Ex-VEGF-C-DMH	This paper.	1271*	Production of the cathepsin D-cleaved form of VEGF-C in S2 cells
transfected construct	pMT-hygro-BiPSP-hVEGF-C-FL	This paper.	751*	Production of untagged pro-VEGF-C in S2 cells
transfected construct	pSecTagI-IgKSP-ΔNΔC-hVEGF-C-H6	This paper.	2242*	Production of the plasmin1-cleaved form of VEGF-C (primary plasmin cleavage, between VEGF-C aa 102 and 103)
transfected construct	pSecTagI-IgKSP-ΔNΔC-VEGF-C-ADAMTS3-H6	This paper.	2313*	Production of the ADAMTS3-cleaved form of VEGF-C (cleavage between aa residues 111 and 112)
transfected construct	pSecTagI-IgKSP-ΔNΔC-VEGF-C-KLK3-H6	This paper.	2312*	Production of the KLK3-cleaved form of VEGF-C (cleavage between aa residues

				114 and 115)
transfected construct	pSecTagI-IgKSP-ΔNΔC-VEGF-C-CATD-H6	This paper.	2315*	Production of the cathepsin D-cleaved form of VEGF-C (cleavage between aa residues 119 and 120)
transfected construct	pSecTagI-IgKSP-ΔNΔC-VEGF-C-plasmin2-H6	This paper.	2314*	Production of the plasmin2-cleaved form of VEGF-C (secondary plasmin cleavage, between VEGF-C aa 127 and 128)
transfected construct	pSecTagI-IgKSP-ΔNΔC-VEGF-C(C156S)-H6	This paper.	2318*	Production of the mature form of the VEGF-C-C156S mutant (primary plasmin cleavage, between VEGF-C aa 102 and 103)
transfected construct	pMX-hCCBE1-StrIII	(Jeltsch et al., 2014)	1494*	Production of full-length CCBE1
transfected construct	psubCAG-WPRE-IgKSP-ΔNΔC-hVEGF-C-KLK3	This paper.	2380*	Generation of recombinant adeno-associated virus
transfected construct	psubCAG-WPRE-IgKSP-ΔNΔC-hVEGF-C-CATD	This paper.	2351*	Generation of recombinant adeno-associated virus
transfected construct	psubCMV-WPRE-IgKSP-ΔNΔC-hVEGF-C-ADAMTS3	(Anisimov et al., 2009)		Generation of recombinant adeno-associated virus (positive control)
transfected construct	psubCMV-WPRE	(Paterna et al., 2000)		Generation of recombinant adeno-associated virus (negative control)
transformed construct	pFB1-melSP-hVEGF-D-FL-H6	This paper and (Achen et al., 1998)	229*	Generation of recombinant baculovirus (FastBac system)
transformed construct	pFB1-melSP-ΔNΔC-hVEGF-D-H6	This paper and (Achen et al., 1998)	118*	Generation of recombinant baculovirus (FastBac system)
biological sample (*H. sapiens*)	human saliva	collected from authors of this paper		
biological sample (*H. sapiens*)	human seminal plasma	collected from authors of this paper		
antibody	anti-VEGF-C antiserum, rabbit polyclonal	(Baluk et al., 2005)	AS no. 6	WB (1:2000)
antibody	anti-VEGF-C antiserum, rabbit polyclonal	(Joukov et al., 1997)	AS 882	WB (1:1000) IP (1:500-1:1000)
antibody	anti-VEGF-C antiserum, rabbit	(Joukov et al., 1997)	AS 905	WB (1:500)

	polyclonal			
antibody	anti-VEGF-C antiserum, rabbit polyclonal	This paper.	AS 885	WB (1:250)
antibody	anti-VEGF-C antiserum, rabbit polyclonal	This paper.	AS 890	WB (1:250)
antibody	anti-VEGF-C antiserum, rabbit polyclonal	This paper.	AS no. 3/4	WB (1:1000)
antibody	anti-VEGF-C antibody, rabbit polyclonal	Abcam	RRID:AB_2241408	WB (1:1000)
antibody	anti-VEGF-C antibody, rabbit polyclonal	Abcam	ab135506	WB (1:1000)
antibody	anti-VEGF-C antibody, rabbit polyclonal	Novus/ Biotechne	NB110-61022	WB (1:1000)
antibody	anti-VEGF-C antibody, rabbit polyclonal	Cell Signaling Technology	RRID:AB_2213314	WB (1:1000)
antibody	anti-VEGF-C antibody, rabbit polyclonal	Invitrogen/ ThermoFisher	RRID:AB_2547246	WB (1:500)
antibody	anti-VEGF-C antibody, rabbit polyclonal	Sigma-Aldrich/ Merck	SAB1303101	WB (1:500)
antibody	anti-VEGF-C antibody, rabbit polyclonal	Sigma-Aldrich/ Merck	SAB1303607	WB (1:500)
antibody	anti-VEGF-C antibody, goat polyclonal	R&D Systems/ Biotechne	RRID:AB_2241406	WB (1:1000)
antibody	anti-VEGF-C antibody, mouse monoclonal	Santa Cruz Biotechnology	RRID:AB_11012156	WB (1:500)
antibody	anti-VEGF-C antibody, mouse	Santa Cruz Biotechnology	RRID:AB_1131232	WB (1:500)

	monoclonal			
antibody	anti-VEGF-C antibody, mouse monoclonal	R&D Systems/ Biotechne	RRID:AB_2213313	WB (1:500)
antibody	anti-VEGF-C antibody, mouse monoclonal	Invitrogen/ ThermoFisher	RRID:AB_2725653	WB (1:200)
antibody	anti-VEGF-C antibody, mouse monoclonal	Sigma-Aldrich/ Merck	SAB1306762	WB (1:100)
antibody	anti-KLK3 antibody, mouse monoclonal	(Stenman et al., 1999)	5C7	neutralization at 2-fold molar excess
antibody	anti-VEGF-D, goat polyclonal	R&D Systems/ Biotechne	RRID:AB_355293	WB (1:1000)
antibody	anti-phosphotyrosine antibody 4G10, mouse monoclonal	Millipore/ Merck	RRID:AB_309678	WB (1:5000)
antibody	anti-VEGFR-2, goat polyclonal	R&D Systems/ Biotechne	RRID:AB_355320	WB (1:1500)
antibody	anti-VEGFR-3, mouse monoclonal	(Dumont et al., 1998)	9D9F9	WB (1:1000)
antibody	anti-CCBE1, rabbit polyclonal	Atlas Antibodies/ Sigma-Aldrich/ Merck	RRID:AB_10794515	WB (1:1000)
antibody	Penta·His Antibody, mouse monoclonal	Qiagen	RRID:AB_2619735	WB (1:1500)
antibody	anti-mouse Lyve-1, rabbit polyclonal	(Karkkainen et al., 2003)		IF (1:1000)
antibody	anti-mouse CD31, rat monoclonal	BD Biosciences	RRID:AB_393571	IF (1:500)
antibody	HRP-conjugated Strep-Tactin	IBA	2-1502-001	1:100000
antibody	Donkey anti-goat IgG	Jackson Immuno Research	RRID:AB_2340390	1:2500
antibody	Goat anti-mouse IgG	Jackson Immuno Research	RRID:AB_10015289	1:2500
antibody	Goat anti-rabbit IgG	Jackson Immuno Research	RRID:AB_2313567	1:2500
antibody	Alexa 488 donkey anti-rat	Molecular Probes/Thermo Fisher	RRID:AB_2535794	1:500
antibody	Alexa 594 donkey anti-rabbit	Molecular Probes/Thermo Fisher	RRID:AB_141637	1:500
recombinant protein	KLK3	(Wu et al., 2004;		isoform B

		Zhang et al., 1995)		
recombinant protein	Cathepsin D (CATD)	R&D Systems/ Biotechne	1014-AS	
recombinant protein	pro-VEGF-C	This paper.	751*	untagged pro-VEGF-C
recombinant protein	ΔNΔC-VEGF-C or mature VEGF-C	(Kärpänen et al., 2006)	792*	C-terminally histagged mature human VEGF-C (minor form)
recombinant protein	VEGF-C_{DMH}	This paper.	2454*	DMH form of human VEGF-C expressed in S2 cells
recombinant protein	pro-VEGF-D	(Achen et al., 1998)	229*	C-terminally histagged human pro-VEGF-D
recombinant protein	ΔNΔC-VEGF-D or mature VEGF-D	(Achen et al., 1998)	118*	C-terminally histagged mature human VEGF-D (major form)
recombinant protein	CCBE1-StrepIII	(Jeltsch et al., 2014)	1494*	StrepIII-tagged human CCBE1 protein
recombinant protein	VEGFR-3/Fc	(Jeltsch et al., 2006)	810*	human VEGFR-3 extracellular domains 1-7 fused to IgG1Fc
recombinant protein	VEGFR-2/Fc	(Leppänen et al., 2013, 2010)	321*	human VEGFR-2 extracellular domains 1-3 fused to IgG1Fc
commercial assay or kit	Human VEGF-C Quantikine ELISA Kit	R&D Systems/ Biotechne	DVEC00	
chemical compound, drug	streptactin resin/sepharose	IBA	2-1201-010	
chemical compound, drug	Protein A-Sepharose-4B beads CL-4B (PAS)	GE Healthcare	17-0780-01	
chemical compound, drug	Chelex 100	Bio-Rad	1421253	
chemical compound, drug	cOmplete	Roche	11697498001	
other	VECTASHIELD mounting medium with DAPI	Vector Laboratories	RRID:AB_2336790	nuclei label

439 * The asterisk denotes internal lab numbering of the corresponding DNA prep.

440 **Protein Production and Purification**

441 KLK3 (isoform B) was purified by immunoaffinity chromatography from pooled seminal plasma
442 (Wu et al., 2004). The separation of the different isoforms by anion-exchange chromatography was
443 performed as described (Zhang et al., 1995). For the production of untagged pro-VEGF-C, full-
444 length human VEGF-C cDNA was cloned into the Drosophila expression vector pMT-BiP
445 (Invitrogen/Thermo Fisher Scientific, Waltham, MA). The protein was expressed in stably-

transfected S2 cells in Insect-Xpress medium (Lonza, Basel, Switzerland) supplemented with 250 µg/ml hygromycin at 26°C. The cells were induced with 1mM $CuSO_4$ and the conditioned medium was harvested 4 days post-induction. VEGF-C was purified from the conditioned medium by Heparin affinity chromatography (HiTrap Heparin HP, GE Healthcare, Chicago, IL) at pH 6.7, followed by cation exchange chromatography over a MonoS or HiTrap SP HP column (GE Healthcare) at the same pH and gel filtration on a Superdex 200 Increase (GE Healthcare) column in PBS. C-terminally his-tagged pro-VEGF-D was produced with the baculovirus system as described (Achen et al., 1998). Purification was performed by affinity chromatography over Excel sepharose (GE Healthcare), followed by gel filtration as described for pro-VEGF-C. C-terminally his-tagged mature VEGF-D was produced from a truncated cDNA analogous to pro-VEGF-D. CCBE1 protein was produced and purified as described (Jeltsch et al., 2014). Similarly, human VEGFR-3/Fc (containing extracellular domains 1-7) and VEGFR-2/Fc (containing extracellular domains 1-3) were purified as described (Jeltsch et al., 2006; Leppänen et al., 2013, 2010).

Recombinant Adeno-Associated Viral Vector Production

Recombinant Adeno-Associated Viruses (AAVs) were produced as previously described (Jeltsch et al., 2014).

Cell lines

Stably transfected cell lines were obtained directly from the generating laboratories (indicated by the reference in the key resource table) and other cell lines were obtained from the indicated vendors, who authenticate and monitor for mycoplasma status of these products according to applicable regulations.

Antibodies

All anti-VEGF-C antibodies are listed in the Supplementary File 1. We used further the following antibodies: anti-phosphotyrosine antibody 4G10 (Merck/Millipore), anti-VEGFR-3 antibody sc-321 (Santa Cruz Biotechnology, Dallas, TX), anti-VEGFR-2 (AF357, R&D Systems), anti-VEGF-D (AF286, R&D Systems), anti-CCBE1 (HPA041374, Atlas Antibodies/Sigma-Aldrich/Merck), and Penta-His antibody (#34660, Qiagen, Hilden, Germany).

For the immunofluorescence, the primary antibodies anti-CD31 (BD Biosciences) and anti-Lyve-1 (Karkkainen et al., 2003) were detected using the appropriate Alexa Fluor 488 and 594 secondary antibody conjugates (Molecular Probes/Invitrogen). Antiserum (AS) no. 3/4, AS 885 and AS 890 were generated like AS no. 6 (Baluk et al., 2005), except that mature VEGF-C (Kärpänen et al., 2006) was used as the antigen instead of pro-VEGF-C for AS no. 3/4, and peptide antigens (see Supplementary Table 1 for details) for AS 885 and AS 890.

Activation of pro-VEGF-C and pro-VEGF-D by KLK3

0.94 μg of purified KLK3 was incubated with 1.7 μg of recombinant growth factor in TBS pH 7.7 at 37°C for 24 hours, if not differently indicated. For blocking, the monoclonal antibody against KLK3, 5C7 (Stenman et al., 1999) was used in 2-fold molar excess and the cleavage was analyzed by SDS-PAGE/Western using antiserum 6 and ¾ (VEGF-C) and AF286 (VEGF-D, R&D Systems, Minneapolis, MN). For CCBE1-enhanced cleavage experiments, 10 μl CCBE1-StrepIII (equal to the amount of CCBE1 purified from 12.5 ml of conditioned 293T medium) were included in the reaction.

Activation of VEGF-C and VEGF-D by cathepsin D

80 µg of pro-VEGF-C/pro-VEGF-D in 240 µl PBS or ΔNΔC-VEGF-C/ΔNΔC-VEGF-D in 60 µl PBS were incubated with the same volume of human, recombinant cathepsin D, which had been activated and diluted according to the instructions of the manufacturer (1014-AS, R&D Systems). Incubation was performed at 37°C, and aliquots were taken at 15 min, 1 h, 4 h and 16 h and frozen at -80°C until analysis. Samples were resolved by reducing SDS-PAGE and proteins were visualized by Coomassie Blue staining. The activation of pro-VEGF-D and ΔNΔC-VEGF-D was visualized by Western blotting.

Transfections, Metabolic Labeling

293T and CHO cell transfections and procedures were performed as described (Jeltsch et al., 2014).

Edman degradation

For the N-terminal sequence analysis, the digestion mixture of purified KLK3 and recombinant pro-VEGF-C or purified protein was resolved by SDS-PAGE and blotted to a PVDF membrane using 1xCAPS buffer/10% methanol. The membrane was Coomassie-stained and the band at 20 kDa was excised after destaining with 50% methanol. Edman degradation was performed using a Procise 494 HT sequencer (Applied Biosystems/Thermo Fisher Scientific) and data analyzed with the Sequence Pro software. Multiple N-termini were disambiguated by a fuzzpro search (Rice et al., 2000) of the major peaks against the VEGF-C and KLK3 sequences and eliminating results incompatible with the molecular weight observed on the gel.

Ba/F3-VEGFR/EpoR Assays

The Ba/F3-hVEGFR-3/EpoR (Achen et al., 2000) and Ba/F3-mVEGFR-2/EpoR (Stacker et al.,

1999b) bioassays were performed with recombinant proteins as described (Mäkinen et al., 2001).

VEGF-C activation in seminal plasma

Fresh ejaculates, showing normal sperm parameters (Cooper et al., 2010), were collected from healthy volunteers among the authors (three different individuals) in full agreement with local regulations and institutional oversight. For analysis by SDS-PAGE/Western blotting, seminal plasma was separated from the cellular fraction and debris after approximately 30 minutes of liquefaction at RT by centrifuging twice for 10 minutes (at 1000g and 10000g). Seminal plasma was stored at -80°C until further analyses. Prior to analysis, thawed seminal plasma samples were sonicated and centrifuged again for 10 minutes at 16000g at 4°C. The upper white layer was discarded and the clear fraction was collected for analyses.

To test the effects of divalent cation concentration and pH on the cleavage of VEGF-C in seminal plasma, 50 mg of Chelex 100 Resin (Bio-Rad, Hercules, CA), 10 µl 0.5M EDTA , or 25 µl 0.1M citric acid were added during the initial liquefaction to each ml of seminal fluid, and samples were incubated for 24 hours at 37°C before continuing with the centrifugation steps.

To slow the proteolytic liquefaction cascade, fresh ejaculates were immediately transferred to ice and a protease inhibitor cocktail (cOmplete, Roche) pre-dissolved in PBS was added at twice the recommended final concentration. Two centrifugation steps of 10000g were performed at 4°C to separate the cellular and gel fraction from the liquid phase and samples were stored at -80°C until further analysis. Before the gel fraction was loaded, it was incubated at 37°C until liquefaction.

Immunoprecipitation, SDS-PAGE, Western blotting and protein analysis

For precipitation with antibodies or soluble receptors, the seminal plasma samples (processed as

described above) were diluted 1+1 with PBS and incubated with 30 µl protein A-Sepharose-4B beads and the respective antibody or soluble receptor overnight at 4°C. The beads were washed 3 times with PBS/0.05% Tween-20 and the bound proteins were eluted by adding 30 µl of 2X Laemmli standard buffer (LSB) followed by heating at 95°C for 10 minutes. For direct loading of proteins (digestion analysis of VEGF-C and VEGF-D, CCBE1 from seminal plasma), 2x or 5x LSB was added to the samples prior to boiling. For Western blotting, proteins were resolved on SDS-PAGE, transferred to PVDF membranes, blocked with 5% BSA in TBS-T for 1 h and probed overnight with the relevant primary antibodies. The membranes were incubated with the appropriate HRP-conjugated secondary antibodies (Jackson Immuno Research, Cambridgeshire, UK, anti-rabbit IgG (111-035-003), anti-mouse IgG (115-035-003) or anti-goat IgG (705-035-003), 1:2500 in 5% skimmed milk in TBS-T) for 1 hour at RT and bands were visualized with ECL plus Western Blotting Substrate (Pierce/Thermo Fisher Scientific, Waltham, MA) or SuperSignal West Femto Maximum Sensitivity Substrate (Pierce/Thermo Fisher Scientific) using the LI-COR Odyssey Fc or cDigit Imaging System (Li_COR, Lincoln, NE). Direct visualization of proteins in the PAGE gels was performed by Coomassie Blue or silver staining.

ELISA

The level of VEGF-C in seminal plasma (processed as described above) was estimated using the Human VEGF-C Quantikine ELISA Kit (DVEC00, R&D Systems) following the manufacturer's instructions.

Stimulation of VEGFR-3 and VEGFR-2 Phosphorylation

Near confluence, PAE cells expressing strep-tagged VEGFR-3 (Leppänen et al., 2013) or VEGFR-2 (Anisimov et al., 2013) were washed with PBS and starved for 4-5 h in DMEM. PAE cells

expressing untagged VEGFR-3 or VEGFR-2 starved for 16 h in DMEM/0.1% BSA were used to analyze N-terminally truncated VEGF-Cs. The cells were stimulated for 10 min with sonicated centrifugation-cleared seminal plasma diluted 1+1 with PBS (as described above), 20 ng/ml ΔNΔC-VEGF-C (Kärpänen et al., 2006) or equimolar amounts of N-terminally truncated VEGF-Cs (adjusted after quantification of VEGF-C levels in conditioned supernatant after transient transfection of CHO cells) to detect phosphorylation of VEGFR-3 and VEGFR-2. Then, the cells were washed twice with ice-cold PBS, lysed with modified RIPA buffer (50 mM Tris-HCl pH 8, 0.5% NP-40, 0.5% Triton X-100, EDTA-free protease inhibitor cocktail (cOmplete, Roche, Pleasanton, CA), 0.1 mM PMSF, 1 mM Na_3VO_4, and 1 mM NaF). VEGFR-3 and VEGFR-2 were precipitated from the cell lysate using Strep-Tactin Sepharose (IBA, Göttingen, Germany) for strep-tagged VEGFR-2/-3 or immunoprecipitated using protein A Sepharose (PAS) and anti-VEGFR-3 (clone 9D9F9, (Dumont et al., 1998)) or anti-VEGFR-2 (AF357, R&D Systems), washed 3 times with PBS/0.05% Tween-20/1mM Na_3VO_4 and eluted with 2x Laemmli buffer and analyzed by SDS-PAGE/Western blot using the phospho-tyrosine-specific antibody 4G10 (Merck/Millipore, Darmstadt, Germany, 1:5000). Membranes were stripped using Re-Blot plus strong solution (Merck/Millipore) and re-probed with HRP-conjugated Strep-Tactin (IBA, 1:100000), anti-VEGFR-3 (9D9F9) or anti-VEGFR-2 (AF357) to verify equal loading.

Fractionation of human saliva and VEGF-C cleavage activity assay

7 ml of filter-sterilized saliva collected from volunteers among the authors in agreement with local regulations was diluted 1+2 with running buffer (20 mM sodium acetate, pH 4.67) and loaded onto a MonoS column (GE Healthcare). After washing with running buffer, elution was performed with a linear 0-1M NaCl gradient and 1 ml fractions were collected. 20 µl of each fraction were diluted 1+4 with running buffer and 1.3 µg of pro-VEGF-C was added. After 36 h incubation at 37°C, a

Ba/F3-VEGFR-3/EpoR assay was performed with the samples.

Interspecies analysis of VEGF-C sequences

Amino acid sequences of 40 VEGF-C orthologs representing all major vertebrate groups (fish, amphibians, reptiles, birds, mammals) were retrieved via a blastp search against human VEGF-C (UniProtKB P49767). To analyze clade-specific differences in the sequence context of the VEGF-C-activating cleavage, the sequences were truncated to include only sequences corresponding to human VEGF-C amino acids 55 to 228 (i.e. from the center of the N-terminal propeptide to the end of the VEGF homology domain). Alignment was performed with m_coffee (Wallace et al., 2006) and the sequences attached to the tip nodes of a phylogenetic species tree generated by opentree (Hinchliff et al., 2015). The results were rendered with the ETE toolkit (Huerta-Cepas et al., 2016). A Python script of the complete workflow is available from GitHub (Jeltsch, 2018).

Mass spectrometric analysis

Six bands, with identical replicates, were cut from a Coomassie-stained SDS-PAGE gel. Samples were in-gel digested according to the standard protocols and analyzed by LC-ESI-MS/MS using the LTQ Orbitrap Velos Pro mass spectrometer (Thermo Fisher Scientific). The data files were searched for protein identification using Proteome Discoverer 1.4 software (Thermo Fisher Scientific) connected to a server running Mascot 2.4.1 (Matrix Science, Boston, MA). Data were searched against the SwissProt database (release 2014_01). The following search parameters were used: type of search - MS/MS Ion Search, taxonomy - human, enzyme - trypsin, fixed modifications - carbamidomethyl (C), variable modifications - oxidation (M), mass values - monoisotopic, peptide mass tolerance - ± 5 ppm, fragment mass tolerance - ± 0.5 Da, max missed cleavages - 1, instrument type - ESI-TRAP. Only proteins assigned at least with two unique

peptides were accepted.

Cloning

The pMX-hCCBE1-StrIII construct has been described before (Jeltsch et al., 2014). The S2 cell-expression vector pMT-Ex-VEGF-C-DMH was generated by deleting the 51 nucleotides coding for amino acids 103 to 119 of VEGF-C from pMT-Ex-ΔNΔC-VEGF-C-H_6, a modified pMT/BiP/V5-His C vector (Invitrogen/Thermo Fisher Scientific), expressing mature VEGF-C (Kärpänen et al., 2006). pMT-hygro-BiPSP-hVEGF-C-FL (for the production of untagged pro-VEGF-C) was generated by PCR-amplification of sequences corresponding to amino acids 32-419 of VEGF-C and cloning of the product into BglII-opened pMT-BiPV5HisC-hygro, another derivative of pMT/BiP/V5-His C, in which the 260bp SapI-AccI fragment had been replaced by the SapI-AccI hygromycin expression cassette from pCoHygro (Invitrogen/Thermo Fisher Scientific).

pSecTagI-IgKSP-ΔNΔC-hVEGF-C-H_6 (the mammalian vector expressing mature VEGF-C corresponding to VEGF-C activated by plasmin cleavage between VEGF-C amino acids 102 and 103) was constructed by inserting the BamHI/BclI-cut VEGF-C PCR amplification product of primers 5'-GATGCTCGAGGATCCGACAGAAGAGACTATAAAATTTGC-3' and 5'-GCATGATCACAGTTTAGACATGC-3' into the BamHI-opened pMosaic vector (Jeltsch et al., 2006)**.** The cDNAs coding for N-terminally truncated VEGF-C (corresponding to mature VEGF-C forms as activated by KLK3 cleavage, ADAMTS3 cleavage, and plasmin cleavage between amino acid residues 127 and 128) were PCR amplified from pSecTagI-IgKSP-ΔNΔC-hVEGF-C-H_6 using specific forward primers (5'-TCCG GATCCGGATCCAAATACAGAGATCTTGAAAAGTATTGATAATGAGTGG-3'; 5'-TC CGGATCCGGATCCAGCACATTATAATACAGAGATCTTGAAAAGTATTG-3'; and 5'-TCCGGATCCGGATCCAAAGACTCAATGCATGCCACG-3') and the same reverse primer (5'-

ACCTACTCAGACAATGCGATGC-3'), and subcloned into pSecTagI-IgKSP-ΔNΔC-hVEGF-C-H_6 as BamHI-EcoRI fragments. The DMH/CatD form and C156S mutant of VEGF-C were subcloned in the same fashion from pMT-Ex-VEGF-C-DMH and pREP7-VEGF-C-C156S (Joukov et al., 1998) into the same vector (using forward primers 5'-CGGATCCAAAAAGTATTGATAATGAGTGGAGA-3' and 5'-GCGGATCCGACAGAAGAGACTATAAAA-3' and reverse primer 5'-GGAATTCAATGATGATGATGGTGATGCAGTTTAGACATGC-3').

The shuttle vectors to produce pro-VEGF-D (pFB1-melSP-hVEGF-D-FL-H_6) and a mature form of VEGF-D (pFB1-melSP-ΔNΔC-hVEGF-D-H_6) with the baculovirus system were generated by restriction-cloning the BamHI/HindIII-fragments of the PCR products of primers 5'-TGCGGATCCCTCCAGTAATGAACATGGACCAGTGAAGCGATC-3' and 5'-GACAAGCTTAATGATGATGATGGTGATGAGGATTCTTTCGGCTGTGGGGC-3' (for pro-VEGF-D) and 5'-TGCGGATCCGTCAGCATCCCATCGGTCCACTAGGTTTG-3' and 5'-GACAAGCTTAATGATGATGATGGTGATGGGGGGCTGTTGGCAAGCACTTAC-3' (for mature VEGF-D) into a modified pFASTBAC1 vector (Gerhardt et al., 2003).

Cloning of AAV9 constructs

The sequence coding for the Immunoglobulin Kappa signal peptide was amplified using forward primer 5'-CTAAAAGCTGCGGAATTGTACCCGCGGCCGCTAGCGCCACCATGGAGACAGAC-3' and reverse primer 5'-GTCACCAGTGGAACCTGG-3' and the VEGF-C CDS was amplified using forward primer 5'-CTGCTCTGGGTTCCAGGTTCCACTGGTGACAAAAGTATTGATAATGAGTGGAGAAAGA C-3' and reverse primer 5'-

AAATTTTGTAATCCAGAGGTTGATTATCGACGCGTTCAACGTCTAATAATGGAATGAAC T-3'. Both fragments were assembled into a MluI- and NheI-opened and CIPped psubCAG-WPRE vector (Weltner et al., 2012) resulting in psubCAG-WPRE-IgKSP-ΔNΔC-hVEGF-C-CATD. psubCAG-WPRE-IgKSP-ΔNΔC-hVEGF-C-KLK3 was assembled as above, but the reverse primer for the Immunoglobulin Kappa signal peptide CDS amplification was replaced by 5'-TTATCAATACTTTTCAAGATCTCTGTATTGTCACCAGTGGAACCTGG-3' and the forward primer for VEGF-C CDS amplification by 5'-CAATACAGAGATCTTGAAAAGTATTGATAATG-3'.

In vivo experiments

AAV9s (dose of $4x10^{10}$ in 40 µl) encoding negative control, positive control (ADAMTS3-cleaved form of VEGF-C), KLK3-cleaved form of VEGF-C (KLK3-form) and Cathepsin D-cleaved form of VEGF-C (CATD-form) were injected into the Tibialis anterior (TA) muscles of C57Bl/6JRccHsd (Envigo Harlan) female mice . Mice were sacrificed 3 weeks after transduction and the tibialis muscles were harvested. All animal experiments carried out in this study were performed according to guidelines and regulations approved by the National Board for Animal Experiments of the Provincial State Office of Southern Finland .

Histochemistry and Immunofluorescence

Mouse tibialis anterior muscle samples were embedded into Tissue-Tek OCT and frozen in liquid nitrogen-cooled isopentane. 10µm-sections were stained for the lymphatic marker Lyve-1 ((Karkkainen et al., 2003), 1:1000) and blood vascular marker CD31 (BD Biosciences, San Jose, CA, 1:500), followed by Alexa-conjugated secondary antibodies (Molecular Probes/Thermo Fisher Scientific). Nuclei were stained with DAPI with VECTASHIELD (Vector Laboratories, Burlingame, CA). Fluorescent images were obtained with an Axio Imager Z2 upright

epifluorescence microscope (Carl Zeiss AG, Oberkochen, Germany). Images were processed and analysed with Fiji ImageJ (NIH).

RNA extraction and quantitative real time PCR

Muscle tissues were lysed using Trisure reagent (Bioline, London, UK) and the RNA was extracted with Nucleospin RNA II kit (Macherey-Nagel, Düren, Germany). cDNA was synthesized with High-Capacity cDNA Reverse Transcription Kits (Applied Biosystems/Thermo Fisher Scientific) using 1 µg RNA. qRT-PCR was performed with SensiFast SYBR No-ROX Kit (Bioline). All data were normalized to GAPDH. Relative gene expression levels were calculated using the $2^{-\Delta\Delta Ct}$ method. VEGF-C (fwd 5'-TGAACACCAGCACGAGCTAC-3', rev 5'-TCGGCAGGAAGTGTGATTGG-3') and mGAPDH (fwd 5'-ACAACTTTGGCATTGTGGAA-3', rev 5'-GATGCAGGGATGATGTTCTG-3') primers were used for the real time PCR.

Statistical analysis.

Data are presented as mean±SD or mean±SEM. Data were analysed using GraphPad Prism statistical analysis software (Version 8). Data analysis details are mentioned in the respective figure legends.

ACKNOWLEDGMENTS

We thank Tapio Tainola for DNA sequencing, Maria Arrano de Kivikko for technical help with animal experiment, Sini Miettinen from the Proteomics Unit of the Institute of Biotechnology (University of Helsinki, Finland) for protein sequencing, and Anne Rokka from the Turku Proteomics Facility (Turku Centre for Biotechnology, Finland) for the mass spectrometric analysis. We further thank Seppo Kaijalainen for the cloning of the AAV constructs, the Biomedicum

Imaging Unit, Tanja Laakkonen from the AAV Gene Transfer and Cell Therapy Core Facility of Biocenter Finland, and the Laboratory Animal Centre of the University of Helsinki for professional services.

FUNDING SOURCES

The Academy of Finland (grant numbers 265982, 272683, 273612 and 273817) and the Finnish Foundation for Cardiovascular Research are acknowledged for funding. The work in the Dr. Jeltsch's laboratory has been further supported by the Jane and Aatos Erkko Foundation, the Cancer Society of Finland, the Magnus Ehrnrooth Foundation, the K. Albin Johansson Foundation, the Einar and Karin Stroem Foundation for Medical Research and the Päivikki and Sakari Sohlberg Foundation. The Integrated Life Science Doctoral Program and Wihuri Research Institute supported the salary of SKJ, the Finnish-Norwegian Medical Foundation supported KM and the Päivikki and Sakari Sohlberg Foundation supported KR. Biomedicum Helsinki Foundation and Cancer Society of Finland are also acknowledged for their support to SKJ. HK was supported by the Sigrid Jusélius Foundation and Laboratoriolääketieteen edistämissäätiö. The work in Dr. Alitalo's laboratory was funded by the Jane and Aatos Erkko Foundation, European Research Council (ERC) under the European Union's Horizon 2020 research and innovation programme under grant agreement No 743155, the Wihuri Research Institute, maintained by the Jenny and Antti Wihuri Foundation, the Academy of Finland Centre of Excellence Program 2014-2019 (307366), the Novo Nordisk Foundation and the Sigrid Jusélius Foundation.

DISCLOSURES

None.

REFERENCES

Abe H, Al-zi'abi MO, Sekizawa F, Acosta TJ, Skarzynski DJ, Okuda K. 2014. Lymphatic involvement in the disappearance of steroidogenic cells from the corpus luteum during luteolysis. *PLoS One* **9**:e88953.

Achen MG, Jeltsch M, Kukk E, Mäkinen T, Vitali A, Wilks AF, Alitalo K, Stacker SA. 1998. Vascular endothelial growth factor D (VEGF-D) is a ligand for the tyrosine kinases VEGF receptor 2 (Flk1) and VEGF receptor 3 (Flt4). *Proc Natl Acad Sci U S A* **95**:548–553.

Achen MG, Roufail S, Domagala T, Catimel B, Nice EC, Geleick DM, Murphy R, Scott AM, Caesar C, Makinen T, Alitalo K, Stacker SA. 2000. Monoclonal antibodies to vascular endothelial growth factor-D block its interactions with both VEGF receptor-2 and VEGF receptor-3. *Eur J Biochem* **267**:2505–2515.

Anisimov A, Alitalo A, Korpisalo P, Soronen J, Kaijalainen S, Leppänen V-M, Jeltsch M, Ylä-Herttuala S, Alitalo K. 2009. Activated Forms of VEGF-C and VEGF-D Provide Improved Vascular Function in Skeletal Muscle. *Circ Res* **104**:1302–1312.

Anisimov A, Leppanen V-M, Tvorogov D, Zarkada G, Jeltsch M, Holopainen T, Kaijalainen S, Alitalo K. 2013. The basis for the distinct biological activities of vascular endothelial growth factor receptor-1 ligands. *Sci Signal* **6**.

Baluk P, Tammela T, Ator E, Lyubynska N, Achen MG, Hicklin DJ, Jeltsch M, Petrova TV, Pytowski B, Stacker SA, Ylä-Herttuala S, Jackson DG, Alitalo K, McDonald DM. 2005. Pathogenesis of persistent lymphatic vessel hyperplasia in chronic airway inflammation. *J Clin Invest* **115**:247–257.

Benes P, Vetvicka V, Fusek M. 2008. Cathepsin D-many functions of one aspartic protease. *Crit Rev Oncol Hematol* **68**:12–28.

Binder NK, Evans J, Gardner DK, Salamonsen LA, Hannan NJ. 2014. Endometrial signals improve embryo outcome: functional role of vascular endothelial growth factor isoforms on embryo development and implantation in mice. *Hum Reprod* **29**:2278–2286.

Björndahl L, Kvist U. 2003. Sequence of ejaculation affects the spermatozoon as a carrier and its message. *Reprod Biomed Online* **7**:440–448.

Brakenhielm E, Burton JB, Johnson M, Chavarria N, Morizono K, Chen I, Alitalo K, Wu L. 2007. Modulating metastasis by a lymphangiogenic switch in prostate cancer. *Int J Cancer* **121**:2153–2161.

Brown LF*., Yeo K-T, Berse B, Morgentaler A, Dvorak HF, Rosen S. 1995. Vascular permeability factor (vascular endothelial growth factor) is strongly expressed in the normal male genital tract and is present in substantial quantities in semen. *J Urol* **154**:576–579.

Bui HM, Enis D, Robciuc MR, Nurmi HJ, Cohen J, Chen M, Yang Y, Dhillon V, Johnson K, Zhang H, Kirkpatrick R, Traxler E, Anisimov A, Alitalo K, Kahn ML. 2016. Proteolytic activation defines distinct lymphangiogenic mechanisms for VEGFC and VEGFD. *J Clin Invest* **126**:2167–2180.

Burton JB, Priceman SJ, Sung JL, Brakenhielm E, An DS, Pytowski B, Alitalo K, Wu L. 2008. Suppression of prostate cancer nodal and systemic metastasis by blockade of the lymphangiogenic axis. *Cancer Res* **68**:7828–7837.

Byzova TV, Goldman CK, Jankau J, Chen J, Cabrera G, Achen MG, Stacker SA, Carnevale KA, Siemionow M, Deitcher SR, DiCorleto PE. 2002. Adenovirus encoding vascular endothelial growth factor–D induces tissue-specific vascular patterns in vivo. *Blood* **99**:4434–4442.

Chang J-M, Di Tommaso P, Notredame C. 2014. TCS: a new multiple sequence alignment reliability measure to estimate alignment accuracy and improve phylogenetic tree reconstruction. *Mol Biol Evol* **31**:1625–1637.

Cooper TG, Noonan E, Eckardstein S von, Auger J, Baker HWG, Behre HM, Haugen TB, Kruger T, Wang C, Mbizvo MT, Vogelsong KM. 2010. World Health Organization reference values for human semen characteristics. *Hum Reprod Update* **16**:231–245.

Dumont DJ, Jussila L, Taipale J, Lymboussaki A, Mustonen T, Pajusola K, Breitman M, Alitalo K. 1998. Cardiovascular failure in mouse embryos deficient in VEGF receptor-3. *Science* **282**:946–949.

Emami N, Diamandis EP. 2013. Kallikrein-related Peptidases and Semen In: Magdolen V, Sommerhoff, Fritz, Schmitt, editors. Kallikrein-Related Peptidases: Characterization, Regulation, and Interactions

within the Protease Web. Walter de Gruyter. pp. 311–327.
Emami N, Diamandis EP. 2010. Potential role of multiple members of the kallikrein-related peptidase family of serine proteases in activating latent TGF beta 1 in semen. *Biol Chem* **391**:85–95.
Ferrara N, Hillan KJ, Novotny W. 2005. Bevacizumab (Avastin), a humanized anti-VEGF monoclonal antibody for cancer therapy. *Biochem Biophys Res Commun* **333**:328–335.
Fortier AH, Nelson BJ, Grella DK, Holaday JW. 1999. Antiangiogenic activity of prostate-specific antigen. *J Natl Cancer Inst* **91**:1635–1640.
Gerhardt H, Golding M, Fruttiger M, Ruhrberg C, Lundkvist A, Abramsson A, Jeltsch M, Mitchell C, Alitalo K, Shima D, Betsholtz C. 2003. VEGF guides angiogenic sprouting utilizing endothelial tip cell filopodia. *J Cell Biol* **161**:1163–1177.
Grennan AK. 2006. Genevestigator. Facilitating web-based gene-expression analysis. *Plant Physiol* **141**:1164–1166.
Hamrah P, Chen L, Zhang Q, Dana MR. 2003. Novel expression of vascular endothelial growth factor receptor (VEGFR)-3 and VEGF-C on corneal dendritic cells. *Am J Pathol* **163**:57–68.
Hannan NJ, Paiva P, Meehan KL, Rombauts LJF, Gardner DK, Salamonsen LA. 2011. Analysis of fertility-related soluble mediators in human uterine fluid identifies VEGF as a key regulator of embryo implantation. *Endocrinology* **152**:4948–4956.
Hinchliff CE, Smith SA, Allman JF, Burleigh JG, Chaudhary R, Coghill LM, Crandall KA, Deng J, Drew BT, Gazis R, Gude K, Hibbett DS, Katz LA, Laughinghouse HD 4th, McTavish EJ, Midford PE, Owen CL, Ree RH, Rees JA, Soltis DE, Williams T, Cranston KA. 2015. Synthesis of phylogeny and taxonomy into a comprehensive tree of life. *Proc Natl Acad Sci U S A* **112**:12764–12769.
Huerta-Cepas J, Serra F, Bork P. 2016. ETE 3: Reconstruction, analysis, and visualization of phylogenomic data. *Mol Biol Evol* **33**:1635–1638.
Ishii K, Otsuka T, Iguchi K, Usui S, Yamamoto H, Sugimura Y, Yoshikawa K, Hayward SW, Hirano K. 2004. Evidence that the prostate-specific antigen (PSA)/Zn2+ axis may play a role in human prostate cancer cell invasion. *Cancer Lett* **207**:79–87.
ist.medisapiens.com. 2019. . *In Silico Transcriptomics online*. http://ist.medisapiens.com/#ENSG00000142515
Iyibozkurt AC, Balcik P, Bulgurcuoglu S, Arslan BK, Attar R, Attar E. 2009. Effect of vascular endothelial growth factor on sperm motility and survival. *Reprod Biomed Online* **19**:784–788.
Jeltsch M. 2018. VEGFC - A Python script for a interspecies comparative analysis of VEGF-C amino acid sequences using BioPython, t_coffee and the ETE toolkit. Github. https://github.com/mjeltsch/VEGFC. cd16435.
Jeltsch M, Jha SK, Tvorogov D, Anisimov A, Leppänen V-M, Holopainen T, Kivelä R, Ortega S, Kärpanen T, Alitalo K. 2014. CCBE1 enhances lymphangiogenesis via a disintegrin and metalloprotease with thrombospondin motifs-3–mediated vascular endothelial growth factor-C activation. *Circulation* **129**:1962–1971.
Jeltsch M, Karpanen T, Strandin T, Aho K, Lankinen H, Alitalo K. 2006. Vascular endothelial growth factor (VEGF)/VEGF-C mosaic molecules reveal specificity determinants and feature novel receptor binding patterns. *J Biol Chem* **281**:12187–12195.
Jennbacken K, Vallbo C, Wang W, Damber J-E. 2005. Expression of vascular endothelial growth factor C (VEGF-C) and VEGF receptor-3 in human prostate cancer is associated with regional lymph node metastasis. *Prostate* **65**:110–116.
Jha SK, Rauniyar K, Karpanen T, Leppänen V-M, Brouillard P, Vikkula M, Alitalo K, Jeltsch M. 2017. Efficient activation of the lymphangiogenic growth factor VEGF-C requires the C-terminal domain of VEGF-C and the N-terminal domain of CCBE1. *Sci Rep* **7**:4916.
Jodar M, Sendler E, Krawetz SA. 2015. The protein and transcript profiles of human semen. *Cell Tissue Res* **363**:85–96.
Joory KD, Levick JR, Mortimer PS, Bates DO. 2006. Vascular endothelial growth factor-C (VEGF-C) expression in normal human tissues. *Lymphat Res Biol* **4**:73–82.
Joukov V, Kumar V, Sorsa T, Arighi E, Weich H, Saksela O, Alitalo K. 1998. A recombinant mutant vascular endothelial growth factor-C that has lost vascular endothelial growth factor receptor-2 binding,

activation, and vascular permeability activities. *J Biol Chem* **273**:6599–6602.
Joukov V, Pajusola K, Kaipainen A, Chilov D, Lahtinen I, Kukk E, Saksela O, Kalkkinen N, Alitalo K. 1996. A novel vascular endothelial growth factor, VEGF-C, is a ligand for the Flt4 (VEGFR-3) and KDR (VEGFR-2) receptor tyrosine kinases. *EMBO J* **15**:290–298.
Joukov V, Sorsa T, Kumar V, Jeltsch M, Claesson-Welsh L, Cao Y, Saksela O, Kalkkinen N, Alitalo K. 1997. Proteolytic processing regulates receptor specificity and activity of VEGF-C. *EMBO J* **16**:3898–3911.
Kalkunte SS, Mselle TF, Norris WE, Wira CR, Sentman CL, Sharma S. 2009. Vascular endothelial growth factor C facilitates immune tolerance and endovascular activity of human uterine NK cells at the maternal-fetal interface. *J Immunol* **182**:4085–4092.
Karkkainen MJ, Haiko P, Sainio K, Partanen J, Taipale J, Petrova TV, Jeltsch M, Jackson DG, Talikka M, Rauvala H, Betsholtz C, Alitalo K. 2003. Vascular endothelial growth factor C is required for sprouting of the first lymphatic vessels from embryonic veins. *Nat Immunol* **5**:74–80.
Karpanen T, Egeblad M, Karkkainen MJ, Kubo H, Ylä-Herttuala S, Jäättelä M, Alitalo K. 2001. Vascular Endothelial Growth Factor C Promotes Tumor Lymphangiogenesis and Intralymphatic Tumor Growth. *Cancer Res* **61**:1786–1790.
Kärpänen T, Heckman CA, Keskitalo S, Jeltsch M, Ollila H, Neufeld G, Tamagnone L, Alitalo K. 2006. Functional interaction of VEGF-C and VEGF-D with neuropilin receptors. *FASEB J* **20**:1462–1472.
Koistinen HK, Stenman U-H. 2012. PSA (Prostate-Specific Antigen) and other Kallikrein-related Peptidases in Prostate Cancer In: Magdolen V, Sommerhoff CP, Fritz H, Schmitt M, editors. Kallikrein-Related Peptidases . Novel Cancer Related Biomarkers. deGruyter. pp. 61–81.
Korpelainen EI, Karkkainen MJ, Tenhunen A, Lakso M, Rauvala H, Vierula M, Parvinen M, Alitalo K. 1998. Overexpression of VEGF in testis and epididymis causes infertility in transgenic mice: evidence for nonendothelial targets for VEGF. *J Cell Biol* **143**:1705–1712.
Krebs R, Tikkanen JM, Ropponen JO, Jeltsch M, Jokinen JJ, Yla-Herttuala S, Nykanen AI, Lemstrom KB. 2012. Critical role of VEGF-C/VEGFR-3 signaling in innate and adaptive immune responses in experimental obliterative bronchiolitis. *Am J Pathol* **181**:1607–1620.
Kubota Y. 2012. Tumor angiogenesis and anti-angiogenic therapy. *Keio J Med* **61**:47–56.
LeBeau AM, Kostova M, Craik CS, Denmeade SR. 2010. Prostate-specific antigen: an overlooked candidate for the targeted treatment and selective imaging of prostate cancer. *Biol Chem* **391**:333–343.
Leppanen V-M, Jeltsch M, Anisimov A, Tvorogov D, Aho K, Kalkkinen N, Toivanen P, Ylä-Herttuala S, Ballmer-Hofer K, Alitalo K. 2011. Structural determinants of vascular endothelial growth factor-D receptor binding and specificity. *Blood* **117**:1507–1515.
Leppänen V-M, Prota AE, Jeltsch M, Anisimov A, Kalkkinen N, Strandin T, Lankinen H, Goldman A, Ballmer-Hofer K, Alitalo K. 2010. Structural determinants of growth factor binding and specificity by VEGF receptor 2. *Proc Natl Acad Sci U S A* **107**:2425–2430.
Leppänen V-M, Tvorogov D, Kisko K, Prota AE, Jeltsch M, Anisimov A, Markovic-Mueller S, Stuttfeld E, Goldie KN, Ballmer-Hofer K, Alitalo K. 2013. Structural and mechanistic insights into VEGF receptor 3 ligand binding and activation. *Proc Natl Acad Sci U S A* **110**:12960–12965.
Leung DW, Cachianes G, Kuang WJ, Goeddel DV, Ferrara N. 1989. Vascular endothelial growth factor is a secreted angiogenic mitogen. *Science* **246**:1306–1309.
Li D, Xie K, Ding G, Li J, Chen K, Li H, Qian J, Jiang C, Fang J. 2014. Tumor resistance to anti-VEGF therapy through up-regulation of VEGF-C expression. *Cancer Lett* **346**:45–52.
Lieu CH, Tran H, Jiang Z-Q, Mao M, Overman MJ, Lin E, Eng C, Morris J, Ellis L, Heymach JV, Kopetz S. 2013. The association of alternate VEGF ligands with resistance to anti-VEGF therapy in metastatic colorectal cancer. *PLoS One* **8**:e77117.
Lilja H, Ulmert D, Vickers AJ. 2008. Prostate-specific antigen and prostate cancer: prediction, detection and monitoring. *Nat Rev Cancer* **8**:268–278.
Li Y-L, Zhao H, Ren X-B. 2016. Relationship of VEGF/VEGFR with immune and cancer cells: staggering or forward? *Cancer Biol Med* **13**:206–214.
Loffredo S, Staiano RI, Granata F, Genovese A, Marone G. 2014. Immune cells as a source and target of angiogenic and lymphangiogenic factors. *Chem Immunol Allergy* **99**:15–36.

Machnik A, Neuhofer W, Jantsch J, Dahlmann A, Tammela T, Machura K, Park J-K, Beck F-X, Müller DN, Derer W, Goss J, Ziomber A, Dietsch P, Wagner H, van Rooijen N, Kurtz A, Hilgers KF, Alitalo K, Eckardt K-U, Luft FC, Kerjaschki D, Titze J. 2009. Macrophages regulate salt-dependent volume and blood pressure by a vascular endothelial growth factor-C–dependent buffering mechanism. *Nat Med* **15**:545–552.

Mackenzie F, Ruhrberg C. 2012. Diverse roles for VEGF-A in the nervous system. *Development* **139**:1371–1380.

Mäkinen T, Jussila L, Veikkola T, Karpanen T, Kettunen MI, Pulkkanen KJ, Kauppinen R, Jackson DG, Kubo H, Nishikawa S-I, Ylä-Herttuala S, Alitalo K. 2001. Inhibition of lymphangiogenesis with resulting lymphedema in transgenic mice expressing soluble VEGF receptor-3. *Nat Med* **7**:199–205.

Malm J, Hellman J, Hogg P, Lilja H. 2000. Enzymatic action of prostate-specific antigen (PSA or hK3): substrate specificity and regulation by Zn(2+), a tight-binding inhibitor. *Prostate* **45**:132–139.

Mandriota SJ, Jussila L, Jeltsch M, Compagni A, Baetens D, Prevo R, Banerji S, Huarte J, Montesano R, Jackson DG, Orci L, Alitalo K, Christofori G, Pepper MS. 2001. Vascular endothelial growth factor-C-mediated lymphangiogenesis promotes tumour metastasis. *EMBO J* **20**:672–682.

Mann T, Lutwak-Mann C. 2012. Male reproductive function and semen: themes and trends in physiology, biochemistry and investigative andrology. Springer Science & Business Media.

Matsumura M, Bhatt AS, Andress D, Clegg N, Takayama TK, Craik CS, Nelson PS. 2005. Substrates of the prostate-specific serine protease prostase/KLK4 defined by positional-scanning peptide libraries. *Prostate* **62**:1–13.

Mattsson JM, Valmu L, Laakkonen P, Stenman U-H, Koistinen H. 2008. Structural characterization and anti-angiogenic properties of prostate-specific antigen isoforms in seminal fluid. *Prostate* **68**:945–954.

McColl BK, Baldwin ME, Roufail S, Freeman C, Moritz RL, Simpson RJ, Alitalo K, Stacker SA, Achen MG. 2003. Plasmin activates the lymphangiogenic growth factors VEGF-C and VEGF-D. *J Exp Med* **198**:863–868.

Mori R, Dorff TB, Xiong S, Tarabolous CJ, Ye W, Groshen S, Danenberg KD, Danenberg PV, Pinski JK. 2010. The relationship between proangiogenic gene expression levels in prostate cancer and their prognostic value for clinical outcomes. *Prostate* **70**:1692–1700.

Muller YA, Christinger HW, Keyt BA, de Vos AM. 1997. The crystal structure of vascular endothelial growth factor (VEGF) refined to 1.93 A resolution: multiple copy flexibility and receptor binding. *Structure* **5**:1325–1338.

Nitta A, Shirasuna K, Haneda S, Matsui M, Shimizu T, Matsuyama S, Kimura K, Bollwein H, Miyamoto A. 2011. Possible involvement of IFNT in lymphangiogenesis in the corpus luteum during the maternal recognition period in the cow. *Reproduction* **142**:879–892.

Obermair A, Obruca A, Pöhl M, Kaider A, Vales A, Leodolter S, Wojta J, Feichtinger W. 1999. Vascular endothelial growth factor and its receptors in male fertility. *Fertil Steril* **72**:269–275.

Owen DH. 2005. A review of the physical and chemical properties of human semen and the formulation of a semen simulant. *J Androl* **26**:459–469.

Pajusola K, Aprelikova O, Pelicci G, Weich H, Claesson-Welsh L, Alitalo K. 1994. Signalling properties of FLT4, a proteolytically processed receptor tyrosine kinase related to two VEGF receptors. *Oncogene* **9**:3545–3555.

Paterna JC, Moccetti T, Mura A, Feldon J, Büeler H. 2000. Influence of promoter and WHV post-transcriptional regulatory element on AAV-mediated transgene expression in the rat brain. *Gene Ther* **7**:1304–1311.

Pavlopoulou A, Pampalakis G, Michalopoulos I, Sotiropoulou G. 2010. Evolutionary history of tissue kallikreins. *PLoS One* **5**:e13781.

Rauniyar K, Jha SK, Jeltsch M. 2018. Biology of vascular endothelial growth factor C in the morphogenesis of lymphatic vessels. *Front Bioeng Biotechnol* **6**.

Red-Horse K. 2008. Lymphatic vessel dynamics in the uterine wall. *Placenta* **29 Suppl A**:S55–9.

Reynolds LP, Grazul-Bilska AT, Redmer DA. 2000. Angiogenesis in the corpus luteum. *Endocrine* **12**:1–9.

Rice P, Longden I, Bleasby A. 2000. EMBOSS: the European Molecular Biology Open Software Suite. *Trends Genet* **16**:276–277.

913 Rinaldo F, Li J, Wang E, Muders M, Datta K. 2007. RalA regulates vascular endothelial growth factor-C
914 (VEGF-C) synthesis in prostate cancer cells during androgen ablation. *Oncogene* **26**:1731–1738.
915 Rissanen TT, Markkanen JE, Gruchala M, Heikura T, Puranen A, Kettunen MI, Kholová I, Kauppinen RA,
916 Achen MG, Stacker SA, Alitalo K, Ylä-Herttuala S. 2003. VEGF-D is the strongest angiogenic and
917 lymphangiogenic effector among VEGFs delivered into skeletal muscle via adenoviruses. *Circ Res*
918 **92**:1098–1106.
919 Robertson SA, Ingman WV, O'Leary S, Sharkey DJ, Tremellen KP. 2002. Transforming growth factor beta-
920 -a mediator of immune deviation in seminal plasma. *J Reprod Immunol* **57**:109–128.
921 Rogers P. 2008. Endometrial angiogenesis and lymphangiogenesis. *Biol Reprod* **78**:231–231.
922 Rutkowski JM, Ihm JE, Lee ST, Kilarski WW, Greenwood VI, Pasquier MC, Quazzola A, Trono D, Hubbell
923 JA, Swartz MA. 2013. VEGFR-3 neutralization inhibits ovarian lymphangiogenesis, follicle maturation,
924 and murine pregnancy. *Am J Pathol* **183**:1596–1607.
925 Sensabaugh GF. 1978. Isolation and characterization of a semen-specific protein from human seminal
926 plasma: a potential new marker for semen identification. *J Forensic Sci* **23**:106–115.
927 Shaw JLV, Diamandis EP. 2007. Distribution of 15 human kallikreins in tissues and biological fluids. *Clin*
928 *Chem* **53**:1423–1432.
929 Shim AH-R, Liu H, Focia PJ, Chen X, Lin PC, He X. 2010. Structures of a platelet-derived growth
930 factor/propeptide complex and a platelet-derived growth factor/receptor complex. *Proc Natl Acad Sci U*
931 *S A* **107**:11307–11312.
932 Siegfried G, Basak A, Cromlish JA, Benjannet S, Marcinkiewicz J, Chrétien M, Seidah NG, Khatib A-M.
933 2003. The secretory proprotein convertases furin, PC5, and PC7 activate VEGF-C to induce
934 tumorigenesis. *J Clin Invest* **111**:1723–1732.
935 Siemeister G, Marmé D, Martiny-Baron G. 1998. The α-helical domain near the amino terminus is essential
936 for dimerization of vascular endothelial growth factor. *J Biol Chem* **273**:11115–11120.
937 Skobe M, Hawighorst T, Jackson DG, Prevo R, Janes L, Velasco P, Riccardi L, Alitalo K, Claffey K, Detmar
938 M. 2001. Induction of tumor lymphangiogenesis by VEGF-C promotes breast cancer metastasis. *Nat*
939 *Med* **7**:192–198.
940 Spyratos F, Maudelonde T, Brouillet JP, Brunet M, Defrenne A, Andrieu C, Hacene K, Desplaces A,
941 Rouëssé J, Rochefort H. 1989. Cathepsin D: an independent prognostic factor for metastasis of breast
942 cancer. *Lancet* **2**:1115–1118.
943 Stacker SA, Caesar C, Baldwin ME, Thornton GE, Williams RA, Prevo R, Jackson DG, Nishikawa S, Kubo
944 H, Achen MG. 2001. VEGF-D promotes the metastatic spread of tumor cells via the lymphatics. *Nat*
945 *Med* **7**:186–191.
946 Stacker SA, Stenvers K, Caesar C, Vitali A, Domagala T, Nice E, Roufail S, Simpson RJ, Moritz R,
947 Karpanen T, Alitalo K, Achen MG. 1999a. Biosynthesis of vascular endothelial growth factor-D
948 involves proteolytic processing which generates non-covalent homodimers. *J Biol Chem* **274**:32127–
949 32136.
950 Stacker SA, Vitali A, Caesar C, Domagala T, Groenen LC, Nice E, Achen MG, Wilks AF. 1999b. A mutant
951 form of vascular endothelial growth factor (VEGF) that lacks VEGF receptor-2 activation retains the
952 ability to induce vascular permeability. *J Biol Chem* **274**:34884–34892.
953 Stenman U-H, Paus E, Allard WJ, Andersson I, Andrès C, Barnett TR, Becker C, Belenky A, Bellanger L,
954 Pellegrino CM, Børmer OP, Davis G, Dowell B, Grauer LS, Jette DC, Karlsson B, Kreutz FT, van der
955 Kwast TM, Lauren L, Leinimaa M, Leinonen J, Lilja H, Linton HJ, Nap M, Nilsson O, Ng PC, Nustad
956 K, Peter A, Pettersson K, Piironen T, Rapp J, Rittenhouse HG, Rye PD, Seguin P, Slota J, Sokoloff RL,
957 Suresh MR, Very DL, Wang TJ, Wigheden I, Wolfert RL, Yeung KK, Zhang W-M, Zhou Z, Hilgers J.
958 1999. Summary report of the TD-3 workshop: characterization of 83 antibodies against Prostate-
959 Specific Antigen. *Tumor Biology* **20**:1–12.
960 Stief TW. 2007. Thrombin and plasmin activity in semen: *Blood Coagul Fibrinolysis* **18**:386–387.
961 Torry DS, Leavenworth J, Chang M, Maheshwari V, Groesch K, Ball ER, Torry RJ. 2007. Angiogenesis in
962 implantation. *J Assist Reprod Genet* **24**:303–315.
963 Veikkola T, Jussila L, Makinen T, Karpanen T, Jeltsch M, Petrova TV, Kubo H, Thurston G, McDonald
964 DM, Achen MG, Stacker SA, Alitalo K. 2001. Signalling via vascular endothelial growth factor

receptor-3 is sufficient for lymphangiogenesis in transgenic mice. *EMBO J* **20**:1223–1231.
Wallace IM, O'Sullivan O, Higgins DG, Notredame C. 2006. M-Coffee: combining multiple sequence alignment methods with T-Coffee. *Nucleic Acids Res* **34**:1692–1699.
Waltenberger J, Claesson-Welsh L, Siegbahn A, Shibuya M, Heldin CH. 1994. Different signal transduction properties of KDR and Flt1, two receptors for vascular endothelial growth factor. *J Biol Chem* **269**:26988–26995.
Wang C-A, Tsai S-J. 2015. The non-canonical role of vascular endothelial growth factor-C axis in cancer progression. *Exp Biol Med* **240**:718–724.
Webber MM, Waghray A, Bello D. 1995. Prostate-specific antigen, a serine protease, facilitates human prostate cancer cell invasion. *Clin Cancer Res* **1**:1089–1094.
Weltner J, Anisimov A, Alitalo K, Otonkoski T, Trokovic R. 2012. Induced pluripotent stem cell clones reprogrammed via recombinant adeno-associated virus-mediated transduction contain integrated vector sequences. *J Virol* **86**:4463–4467.
Wennemuth G, Schiemann PJ, Krause W, Gressner AM, Aumüller G. 1997. Influence of fibronectin on the motility of human spermatozoa. *Int J Androl* **20**:10–16.
Wu P, Stenman U-H, Pakkala M, Närvänen A, Leinonen J. 2004. Separation of enzymatically active and inactive prostate-specific antigen (PSA) by peptide affinity chromatography. *Prostate* **58**:345–353.
Yang Z-S, Xu Y-F, Huang F-F, Ding G-F. 2014. Associations of nm23H1, VEGF-C, and VEGF-3 receptor in human prostate cancer. *Molecules* **19**:6851–6862.
Zaviacic M, Ablin RJ. 2000. The female prostate and prostate-specific antigen. Immunohistochemical localization, implications of this prostate marker in women and reasons for using the term "prostate" in the human female. *Histol Histopathol* **15**:131–142.
Zhang WM, Leinonen J, Kalkkinen N, Dowell B, Stenman UH. 1995. Purification and characterization of different molecular forms of prostate-specific antigen in human seminal fluid. *Clin Chem* **41**:1567–1573.

Supplementary Material

SUPPLEMENTARY FIGURE LEGENDS

Figure 2-figure supplement 1 and 2. Results of the Edman degradation of KLK3-cleaved pro-VEGF-C.

Because pro-VEGF-C contains already two N-termini due to the intracellular furin cleavage, fuzzpro was used to disambiguate three N-termini. Note that a third, minor KLK3 cleavage site was identified within the VEGF-C silk homology domain.

Figure 2-figure supplement 3. Interspecies analysis of VEGF-C amino acid sequences relevant for activation.

While the VEGF homology domain (VHD) of VEGF-C is highly conserved among all vertebrates, the junction between the VHD and the N-terminal propeptide, which is important for the activation of VEGF-C, shows a significant divergence between different vertebrate clades, especially between most fish clades and the rest of the vertebrates. This divergence could be indicative of differences in the activation of VEGF-C. Note that the tree branches were set to a fixed length for better visual separation; therefore separation along the horizontal axis does not correspond to evolutionary distance. Amino acids were colored (red = high divergence, blue = high conservation) according to the Transitive Consistency Score (Chang et al., 2014). Complete parameters for the analysis can be retrieved from https://github.com/mjeltsch/VEGFC.

Figure 3-figure supplement 1. Comparison of 17 different antibodies for the detection of mature and pro-VEGF-C by Western blotting.

(A) A mixture of equimolar amounts of mature VEGF-C and pro-VEGF-C was resolved on a single-well gel, and a miniblotter (MN20, Immunetics) was used to apply different primary and secondary antibodies during the detection procedure. Each individual slot corresponded to 15 ng of mature VEGF-C (Kärpänen et al., 2006) and 49.3 ng of pro-VEGF-C (Jha et al., 2017). Only 5 of the 17 antibodies recognized both pro-VEGF-C and both form VEGF-C, while 8 antibodies recognized only the inactive pro-VEGF-C. 7 antibodies failed completely to detect any VEGF-C form. Apart from sc-101583 (Santa Cruz Biotechnology), for which no detailed information was available about the antigen, all well-performing antibodies had been raised against a peptide or protein covering the junction between the N-terminal propeptide or the N-terminal end of the VEGF homology domain. However, since differently activated forms of VEGF-C feature different N-

termini, the results of this screening are applicable only to the forms of VEGF-C used in this experiment: the minor (plasmin-generated) form of mature VEGF-C (Joukov et al., 1996) and pro-VEGF-C (also called 29/31-kDa-from) (Joukov et al., 1997). The unknown ratio between pro- and mature VEGF-C in a biological sample precludes the prediction of the net lymphangiogenic potential from an antibody-based VEGF-C signal from any of the antibodies that were tested. Antiserum (AS) no. 6 and monoclonal antibody sc-374628 proved to be in most cases sufficiently sensitive in detecting VEGF-C at physiologically relevant concentrations after immunoprecipitation. Although AS 882 showed a higher sensitivity compared to sc-374628, most experiments were performed with sc-374628 as it generated consistently lower background signal. (B) Peptides and proteins used for the immunization aligned to the VEGF-C amino acid sequences of relevant hosts. Antibodies are shown according to their signal strength from top (high sensitivity) to bottom (no detection). Amino acids differing from the human sequence are highlighted in yellow. All peptide antigens were derived from the human sequence. The amino acid residues covered by the antigens are given in brackets. For protein antigens, the sequence source species are indicated in bold and the expression host in italics if known. Note that the negative result of AS 905 is contrary to published data (Joukov et al., 1997) and might result from suboptimal antibody storage. AS 3/4 was not included in the comparison due to limited amounts available to us, and R&D Systems' AF752 was not included in the comparison since it was raised — differently from all other antibodies tested — in a goat host.

The distinct capabilities to detect specific mature forms of VEGF-C is also seen in Figure 1: AS no. 3/4 detects easily the mature KLK3-form of VEGF-C, whereas AS no.6 shows almost no signal. VEGF-C detection from any biological sample needs to take into account the interaction of pro-VEGF-C with extracellular matrix and cell surface proteins, which may introduce a bias into liquid samples. Similarly, active VEGF-C is a mobile species, potentially introducing a bias into solid

samples as it can be lost during sample preparation. We determined typical seminal plasma VEGF-C levels by ELISA (R&D Systems' DVEC00) as being approximately 2.5 ng/ml VEGF-C (data not shown). However, these results are of limited value, since the calibration of the ELISA is performed using purified mature VEGF-C (minor form), whereas any biological sample will likely contain a mixture of pro-VEGF-C and different forms of mature VEGF-C.

Figure 3-figure supplement 2. The VEGFR-2 phosphorylating activity of seminal plasma is blocked by the VEGF-A-capturing VEGFR-2/Fc fusion protein.

Seminal plasma (diluted 1:1 with PBS) stimulated the phosphorylation of VEGFR-2 expressed in PAE cells. This stimulation was blocked efficiently by VEGFR-2/Fc fusion protein. VEGFR-3/Fc, which captures VEGF-C, but not VEGF-A, is inefficient in blocking the phosphorylation of VEGFR-2.

Figure 3-figure supplement 3. No detection of VEGF-D in seminal plasma.

Liquefied seminal plasma was assayed for VEGF-D using R&D Systems' polyclonal anti-VEGF-D antibody after pull-down with VEGFR-2/IgGFc. VEGF-D was not detected. Unlike for VEGF-C, no extensive screening was performed to identify the antibody with the highest sensitivity and therefore, the presence of VEGF-D at low concentrations (< ~10ng/ml) cannot be excluded.

Figure 4-figure supplement 1. Seminal plasma contains CCBE1 protein.

CCBE1 was detected by Western blotting in both diluted and undiluted seminal plasma samples. Supernatant from 293T cells transfected with CCBE1 was used as a positive control. CCBE1 from 293T cell supernatant presents as a distinct band of approximately 45-50 kDa and its chondroitinylated form as a smear of higher molecular weight (Bui et al., 2016; Jeltsch et al., 2014).

CCBE1 from seminal plasma shows the same lower-size band, but its higher molecular weight forms are more discrete compared to the 293T-produced product. While both seminal plasma CCBE1 and VEGF-C were readily detectable by Western blotting, we were not able to confirm the presence of VEGF-C in seminal plasma by protein mass spectrometry (data not shown). Similarly, a recent mass spec review of seminal proteins does neither identify VEGF-A nor VEGF-C (Jodar et al., 2015). We assume that this inability results from the combined effect of the very broad range of protein concentrations in seminal plasma and the fact that the highly abundant proteins in seminal plasma, like fibronectin and KLK3, are binding VEGF-C, which precludes their specific removal. Protein concentrations in seminal plasma range from values around and above 1 mg/ml for fibronectin (Wennemuth et al., 1997) and KLK3 (Sensabaugh, 1978) down to approximately 2.5 and 10 ng/ml for VEGF-C (this work) and the closely related growth factor VEGF-A (Brown et al., 1995), respectively.

Figure 5-figure supplement 1. Secondary activation of a longer mature VEGF-C form in S2 cells.

(A) Expression of N-terminally truncated VEGF-Cs in transiently transfected CHO cells. Equimolar amounts of VEGF-Cs were calculated based on a densitometric determination of VEGF-C concentrations from a Western blot of conditioned supernatant.

(B) The N-terminally shortest active form of VEGF-C (DMH form) can be expressed from a truncated cDNA. The N-terminal propeptide was deleted to different extents from the VEGF-C cDNA resulting in the expression of mature VEGF-C forms corresponding to the enzymatic activation by different proteases. The C-terminal propeptide was deleted, and following Leu-215, a hexahistidine tag was added to enable comparative quantitation and purification. The cloning process leaves a 6-amino acid residue linker between the Ig Kappa signal peptide and the VEGF-C

cDNA for the 293T cell constructs but only a 2-amino acid residue linker between the BiP signal peptide and the VEGF-C cDNA for the S2 cell constructs. The longer linker of the mammalian DMH construct might be responsible for the inability of the 293T cell-produced VEGF-C_{DMH} to bind to VEGFR-2 and VEGFR-3 (this linker was removed for the generation of the corresponding adeno-associated virus, which induced lymphangiogenesis in skeletal muscle).

(C) In S2 cells, the DMH-form of VEGF-C is generated via proteolytic processing from longer mature forms of VEGF-C (secondary activation). It was detected by N-terminal sequencing of VEGF-C produced by cells transfected with cDNA coding for the N-terminally longest, minor mature form (corresponding to the form generated by the 1st plasmin cleavage). The secondary activation of minor mature form of VEGF-C was more efficient compared to the major mature form of VEGF-C (corresponding to the form generated by ADAMTS3 cleavage).

Figure 6-figure supplement 1. Enrichment and fractionation of VEGF-C cleaving activity.

Sterile-filtered saliva was fractionated using cation exchange chromatography and fractions were analyzed by incubation with pro-VEGF-C, followed by assaying for active VEGF-C using BaF3/VEGFR-3 cells. The three fractions with the highest concentration of active VEGF-C were resolved by SDS-PAGE and six bands were excised for mass spectrometric analysis.

Figure 7-figure supplement 1. Cathepsin D-cleaved pro-VEGF-D stimulates the phosphorylation of VEGFR-2 in PAE cells.

Pro-VEGF-D cleaved by cathepsin D stimulated the phosphorylation of VEGFR-2 expressed in PAE cells at 40 ng/ml and 80 ng/ml concentrations.

Figure 7-figure supplement 2. KLK3/PSA can proteolytically remove both propeptides from VEGF-D.

When VEGF-D is overexpressed in the baculovirus system (A-D), CHO cells (data not shown) or 293 cells (Stacker et al., 1999a), a fraction of the protein does not become proteolytically processed beyond the cleavage of the signal peptide. Before KLK3 cleavage (time = 0), the VEGF-D produced in High Five cells consists of the uncleaved ~50 kDa form and a ~24/26 kDa doublet consisting of the C-terminal propeptide of ~24 kDa and its complement, the N-terminal propeptide and VEGF homology domain (VHD) of ~26 kDa. These sizes are about 5 kDa less compared to the 293-produced VEGF-D and the difference can be traced to the two glycosylation sites within the VHD, which contribute ~8 kDa in the 293 cells, but only ~3 kDa in HighFive cells.

When co-incubated with KLK3, four cleavage products can be detected with an antibody specific for the VEGF homology domain (VHD; AF286, R&D Systems) (A), and two cleavage products can be detected with an antibody detecting the C-terminal hexahistidine tag (B). Based on the published proteolytic processing of VEGF-D (Stacker et al., 1999a), all cleavage products can be assigned based on their size and antibody reactivity to the known forms of VEGF-D (D). The unexpected 34 kDa band has previously been reported when VEGF-D is expressed in 293 cells and was attributed to an additional cleavage site near the C-terminus of C-terminal propeptide (Stacker et al., 1999a) and our data indicate that such cleavage occurs approximately 5 kDa before the end of the VEGF-D polypeptide between the third and forth C-X_{10}-C-X-C-$X_{1,3}$-C repeat. Based on the cleavage specificity of KLK3, the likely cleavage site between the VHD and the C-terminal propeptide is five amino acids shifted (to Tyr-200↓Ser-201) compared to the already described cleavage site (Arg-205↓Ser-206). Both the 34 and the 40 kDa bands disappear upon longer enzyme exposure (data not shown).

KLK3-generated mature VEGF-D is not very well recognized by the VEGF-D antiserum, which is likely due to the fact, that the the antigen used to generate the polyclonal antibody against VEGF-D was produced from a truncated cDNA corresponding to the major mature form of VEGF-D, while the KLK3-generated form misses most of the highly immunogenic N-terminal amino acid residues from the major mature VEGF-D form.

Figure 8-figure supplement 1. Expression of VEGF-C mRNA in tibialis anterior (TA) muscle.

Comparison of VEGF-C mRNA levels in TA muscle transduced with AAV9 encoding for the different forms of mature VEGF-C generated by ADAMTS3 (Pos Ctrl), cathepsin D (CATD-form) and KLK3 (KLK3-form). Data are presented as mean±SEM.

SUPPLEMENTARY FILE LEGENDS

Supplementary File 1. List of anti-VEGF-C antibodies used in this study.

The data for the antibodies in this list were obtained from the product description provided by the supplier. Data missing from suppliers' websites were obtained by direct request to customer support. The dilution refers to what was used for the Western blot analyses performed in this study and is identical to the supplier's recommendation for commercially available antibodies.

Supplementary File 2. Results of mass spectrometric analysis of enriched VEGF-C cleaving activity.

Protein profile of the six samples excised from the SDS-PAGE gel as obtained by LC-ESI-MS/MS analysis.

Source Data Files

Figure 1-Source Data. Ba/F3 assay showing the activity of KLK3-cleaved VEGF-C.

Figure 3-Source Data. Quantification of the ratio of mature VEGF-C to pro-VEGF-C in seminal plasma.

Figure 4-Source Data. Quantification of the ratio of mature VEGF-C to pro-VEGF-C to show that activation of VEGF-C by KLK3 is enhanced by CCBE1.

Figure 5-Source Data. Quantification of VEGFR-3 and VEGFR-2 receptor phosphorylation by N-terminally truncated VEGF-Cs.

Figure 6-Source Data. Quantification of the cleavage of pro-VEGF-C and mature VEGF-C by cathepsin D.

Figure 7-Source Data. Ba/F3 assay showing the receptor-activating properties of cathepsin D-cleaved VEGF-C and VEGF-D.

Figure 8-Source Data. In vivo quantification of lymphangiogenesis and angiogenesis induced by KLK3- and cathepsin D-forms of VEGF-C.

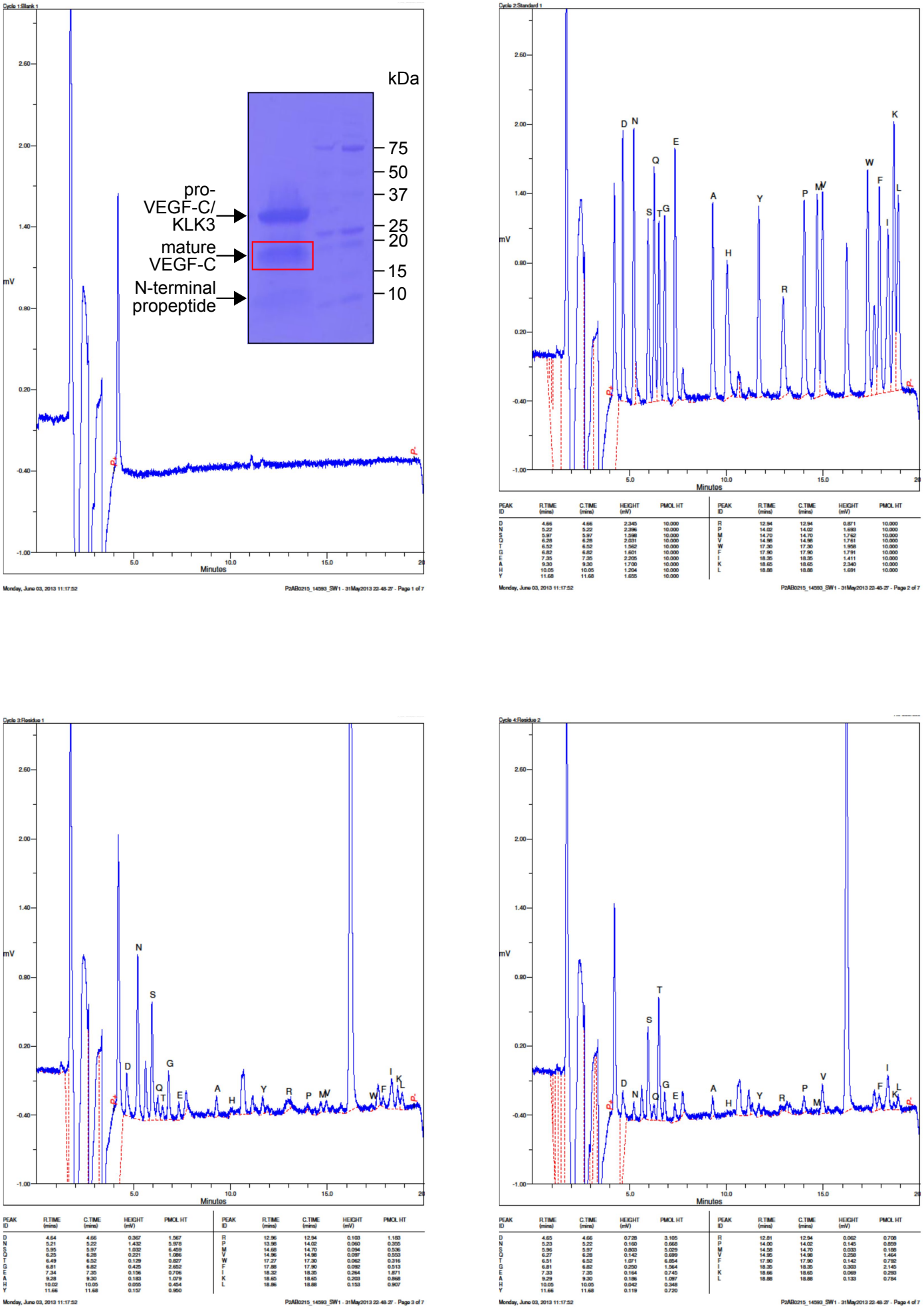

Figure 2-figure supplement 1: Results of Edman degradation of KLK3-cleaved pro-VEGF-C

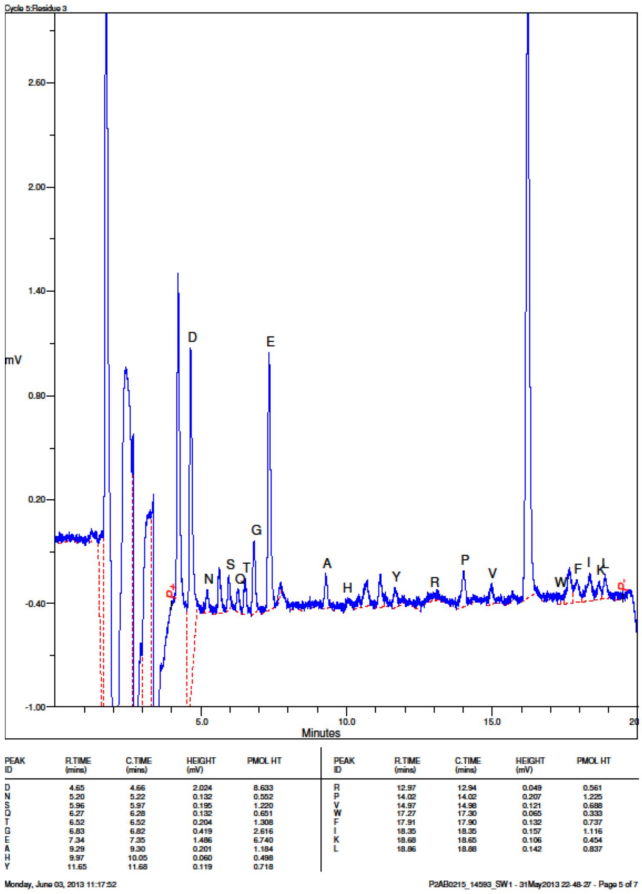

PEAK ID	R.TIME (mins)	C.TIME (mins)	HEIGHT (mV)	PMOL HT
D	4.65	4.66	2.024	8.633
N	5.20	5.22	0.132	0.552
S	5.96	5.97	0.195	1.220
Q	6.27	6.28	0.132	0.651
T	6.52	6.52	0.204	1.308
G	6.83	6.82	0.419	2.616
E	7.34	7.35	1.486	6.740
A	9.29	9.30	0.201	1.184
H	9.97	10.05	0.060	0.498
Y	11.65	11.68	0.119	0.718
R	12.97	12.94	0.049	0.561
P	14.02	14.02	0.207	1.225
V	14.97	14.98	0.121	0.688
W	17.27	17.30	0.065	0.333
F	17.91	17.90	0.132	0.737
I	18.35	18.35	0.157	1.116
K	18.68	18.65	0.106	0.454
L	18.86	18.88	0.142	0.837

Monday, June 03, 2013 11:17:52 — PzAB0215_14593_SW1 - 31May2013 22-48-27 - Page 5 of 7

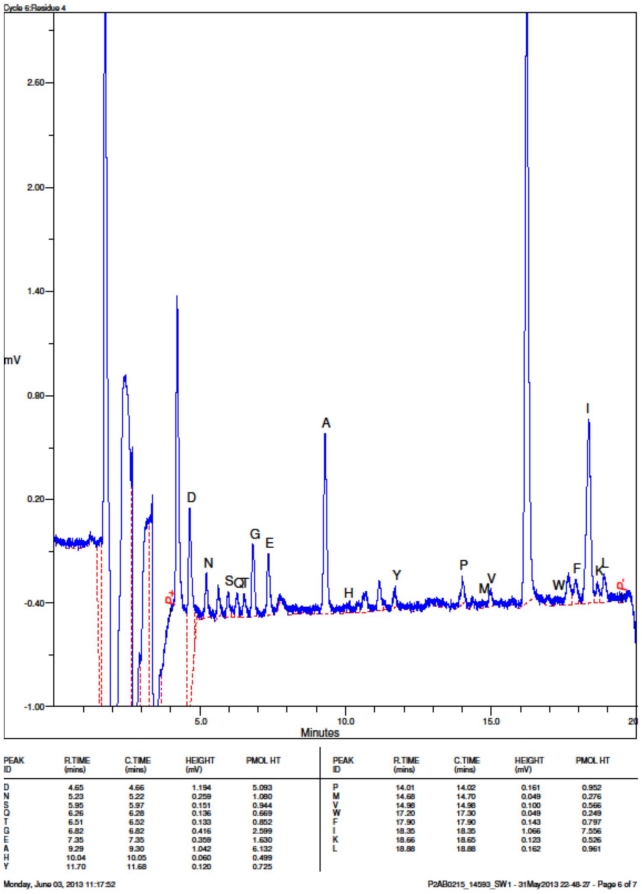

PEAK ID	R.TIME (mins)	C.TIME (mins)	HEIGHT (mV)	PMOL HT
D	4.65	4.66	1.194	5.093
N	5.23	5.22	0.259	1.080
S	5.95	5.97	0.151	0.944
Q	6.26	6.28	0.136	0.669
T	6.51	6.52	0.133	0.852
G	6.82	6.82	0.416	2.599
E	7.35	7.35	0.359	1.620
A	9.29	9.30	1.042	6.132
H	10.04	10.05	0.060	0.499
Y	11.70	11.68	0.120	0.725
P	14.01	14.02	0.161	0.952
M	14.68	14.70	0.049	0.276
V	14.96	14.98	0.100	0.566
W	17.30	17.30	0.049	0.249
F	17.90	17.90	0.143	0.797
I	18.35	18.35	1.066	7.556
K	18.66	18.65	0.123	0.526
L	18.88	18.88	0.162	0.961

Monday, June 03, 2013 11:17:52 — PzAB0215_14593_SW1 - 31May2013 22-48-27 - Page 6 of 7

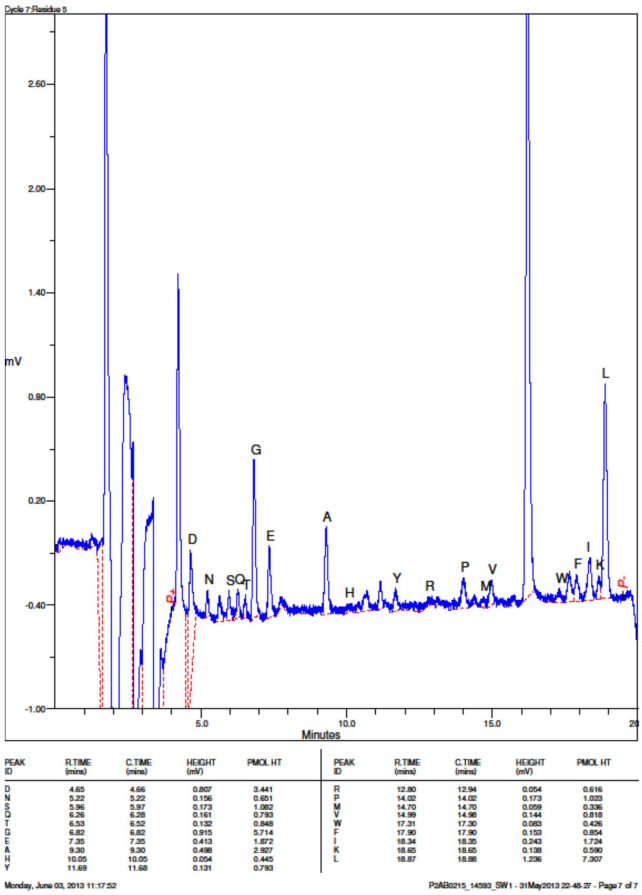

PEAK ID	R.TIME (mins)	C.TIME (mins)	HEIGHT (mV)	PMOL HT
D	4.65	4.66	0.807	3.441
N	5.22	5.22	0.156	0.651
S	5.96	5.97	0.173	1.082
Q	6.26	6.28	0.161	0.793
T	6.53	6.52	0.132	0.846
G	6.82	6.82	0.915	5.714
E	7.35	7.35	0.413	1.872
A	9.30	9.30	0.498	2.927
H	10.05	10.05	0.054	0.445
Y	11.69	11.68	0.131	0.793
R	12.80	12.94	0.054	0.616
P	14.02	14.02	0.173	1.023
M	14.70	14.70	0.059	0.336
V	14.99	14.98	0.144	0.818
W	17.31	17.30	0.083	0.436
F	17.90	17.90	0.153	0.854
I	18.34	18.35	0.243	1.734
K	18.65	18.65	0.138	0.590
L	18.87	18.88	1.206	7.307

Monday, June 03, 2013 11:17:52 — PzAB0215_14593_SW1 - 31May2013 22-48-27 - Page 7 of 7

File: /home/mjeltsch/Documents/Scie...EGFC/ProtSeq/KLK3/disambig.txt Page 1 of 1

protein_sequences.fasta:

```
>sp|P07288|KLK3_HUMAN Prostate-specific antigen OS=Homo sapiens OX=9606 GN=KLK3
PE=1 SV=2
MWVPVVFLTLSVTWIGAAPLILSRIVGGWECEKHSQPWQVLVASRGRAVCGGVLVHPQWV
LTAAHCIRNKSVILLGRHSLFHPEDTGQVFQVSHSFPHPLYDMSLLKNRFLRPGDDSSHD
LMLLRLSEPAELTDAVKVMDLPTQEPALGTTCYASGWGSIEPEEFLTPKKLQCVDLHVI
NDVCAQVHPQKVTKFMLCAGRWTGGKSTCSGDSGGPLVCNGVLQGITSWGSEPCALPERP
SLYTKVVHYRKWIKDTIVANP
>VEGC_HUMAN P49767 Vascular endothelial growth factor C precursor (VEGF-C)
(Vascular endothelial growth factor related protein) (VRP) (Flt4 ligand) (Flt4- L).
MHLLGFFSVACSLLAAALLPGPREAPAAAAAFESGLDLSDAEPDAGEATAYASKDLEEQL
RSVSSVDELMTVLYPEYWKMYKCQLRKGGWQHNREQANLNSRTEETIKFAAAHYNTEILK
SIDNEWRKTQCMPREVCIDVGKEFGVATNTFFKPPCVSVYRCGGCCNSEGLQCMNTSTSY
LSKTLFEITVPLSQGPKPVTISFANHTSCRCMSKLDVYRQVHSIIRRSLPATLPQCQAAN
KTCPTNYMWNNHICRCLAQEDFMFSSDAGDDSTDGFHDICGPNKELDEETCQCVCRAGLR
PASCGPHKELDRNSCQCVCKNKLFPSQCGANREFDENTCQCVCKRTCPRNQPLNPGKCAC
ECTESPQKCLLKGKKFHHQTCSCYRRPCTNRQKACEPGFSYSEEVCRCVPSYWKRPQMS
```

protein_sequences.fuzzpro:

```
#########################################
# Program: fuzzpro
# Rundate: Mon 16 Jul 2018 11:43:46
# Commandline: fuzzpro
#    -pattern "[NS][TS][EDG][AID][GLA]"
#    [-sequence] protein_sequences.fasta
# Report_format: seqtable
# Report_file: protein_sequences.fuzzpro
#########################################

#=======================================
#
# Sequence: VEGC_HUMAN     from: 1   to: 419
# HitCount: 2
#
# Pattern_name Mismatch Pattern
# pattern              0 [NS][TS][EDG][AID][GLA]
#
#=======================================

  Start      End Pattern                          Mismatch Sequence
    115      119 pattern:[NS][TS][EDG][AID][GLA]         . NTEIL
    265      269 pattern:[NS][TS][EDG][AID][GLA]         . SSDAG

#---------------------------------------
#---------------------------------------

#---------------------------------------
# Total_sequences: 2
# Total_length: 680
# Reported_sequences: 1
# Reported_hitcount: 2
#---------------------------------------
```

Figure 2-figure supplement 2: Results of Edman degradation of KLK3-cleaved pro-VEGF-C

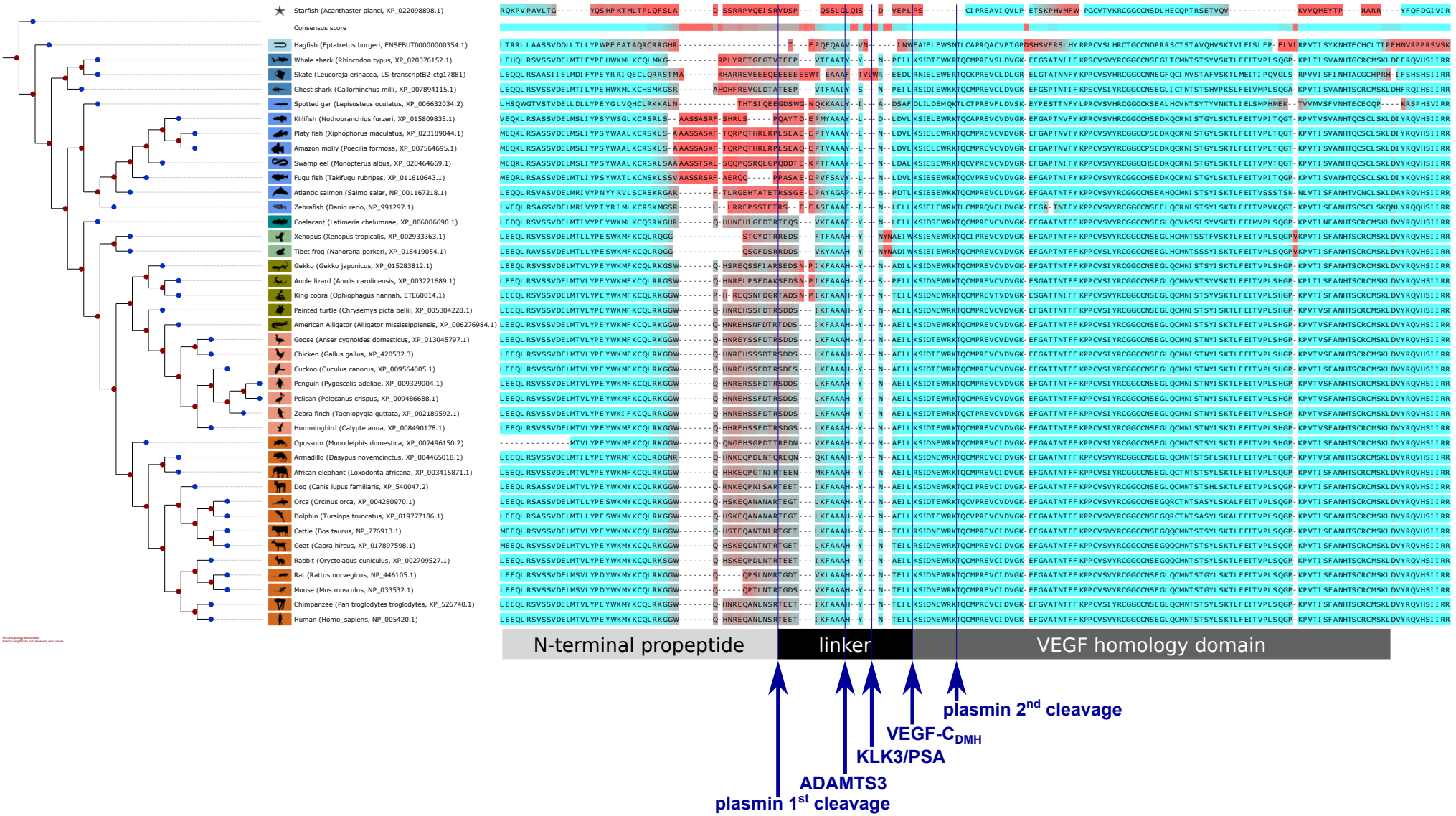

Figure 2-figure supplement 3: Interspecies analysis of VEGF-C amino acid sequences relevant for activation

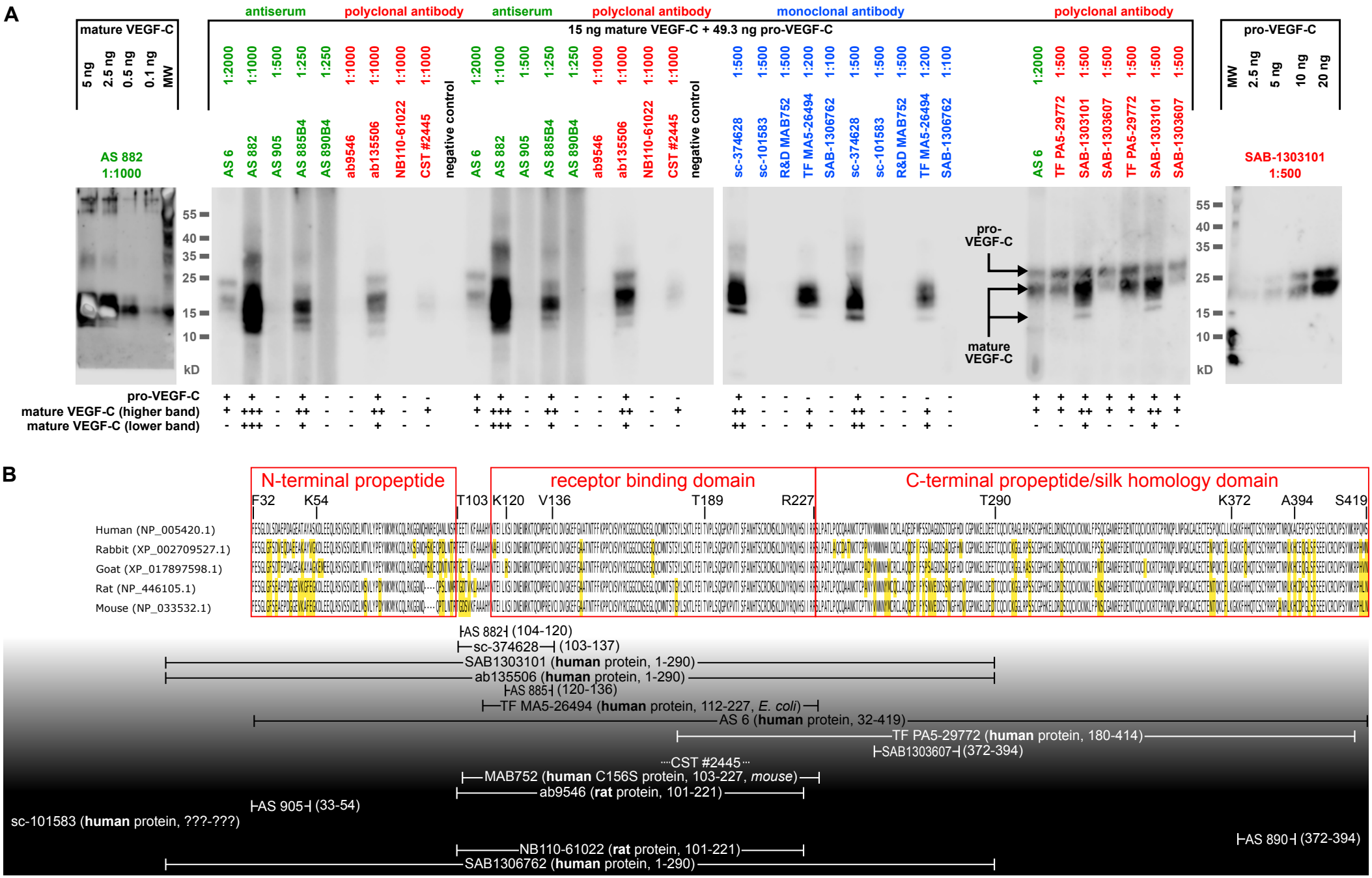

Figure 3-figure supplement 1: Comparison of 17 different antibodies for the detection of mature and pro-VEGF-C by Western blotting

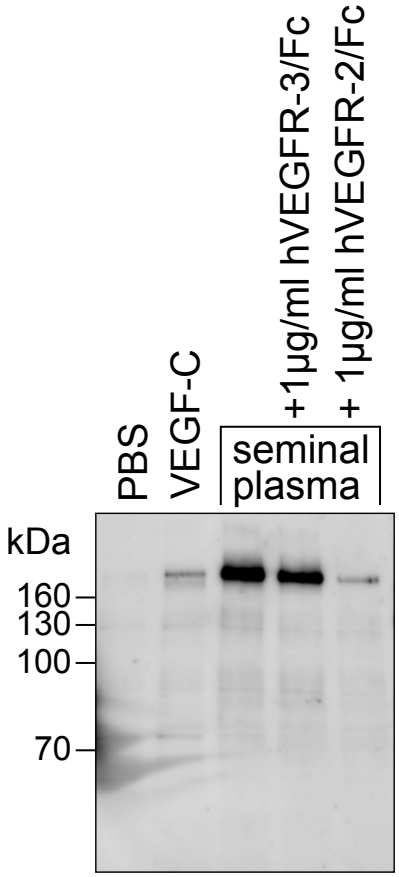

Figure 3-figure supplement 2: The VEGFR-2 phosphorylating activity of seminal plasma is blocked by the VEGF-A-capturing VEGFR-2/Fc fusion protein

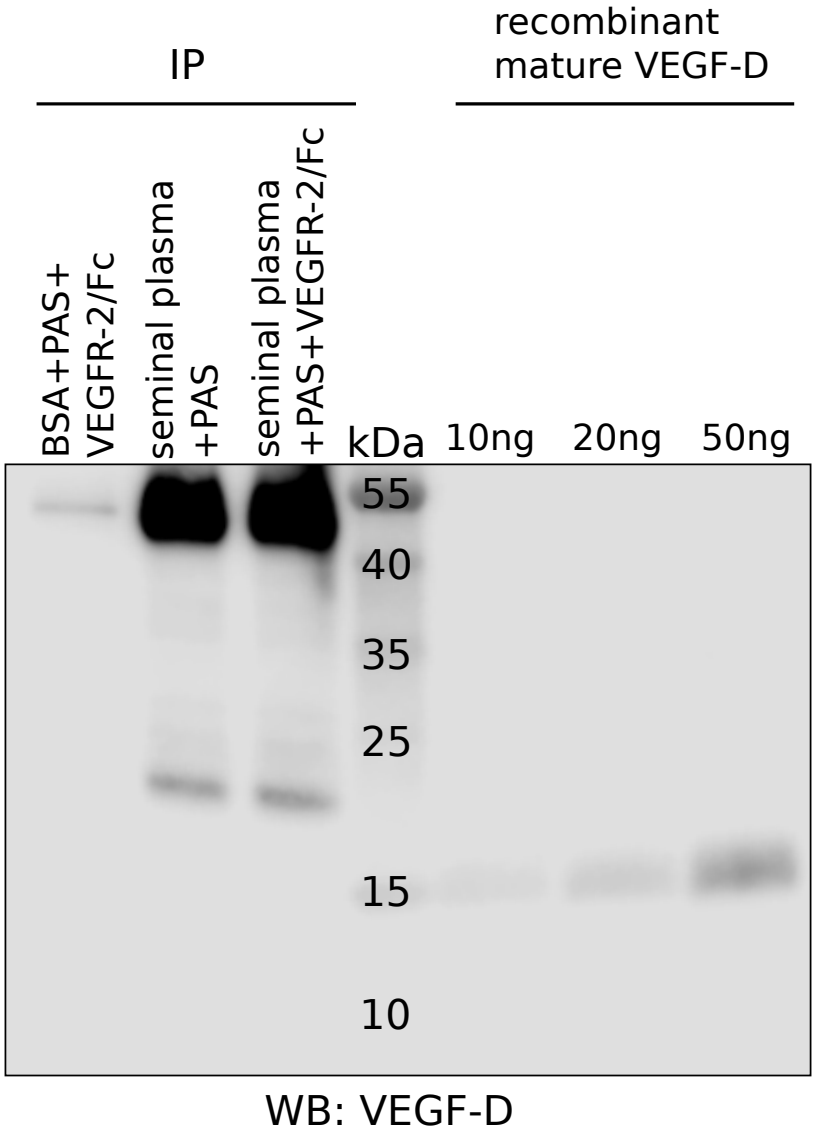

Figure 3-figure supplement 3: No detection of VEGF-D in seminal plasma

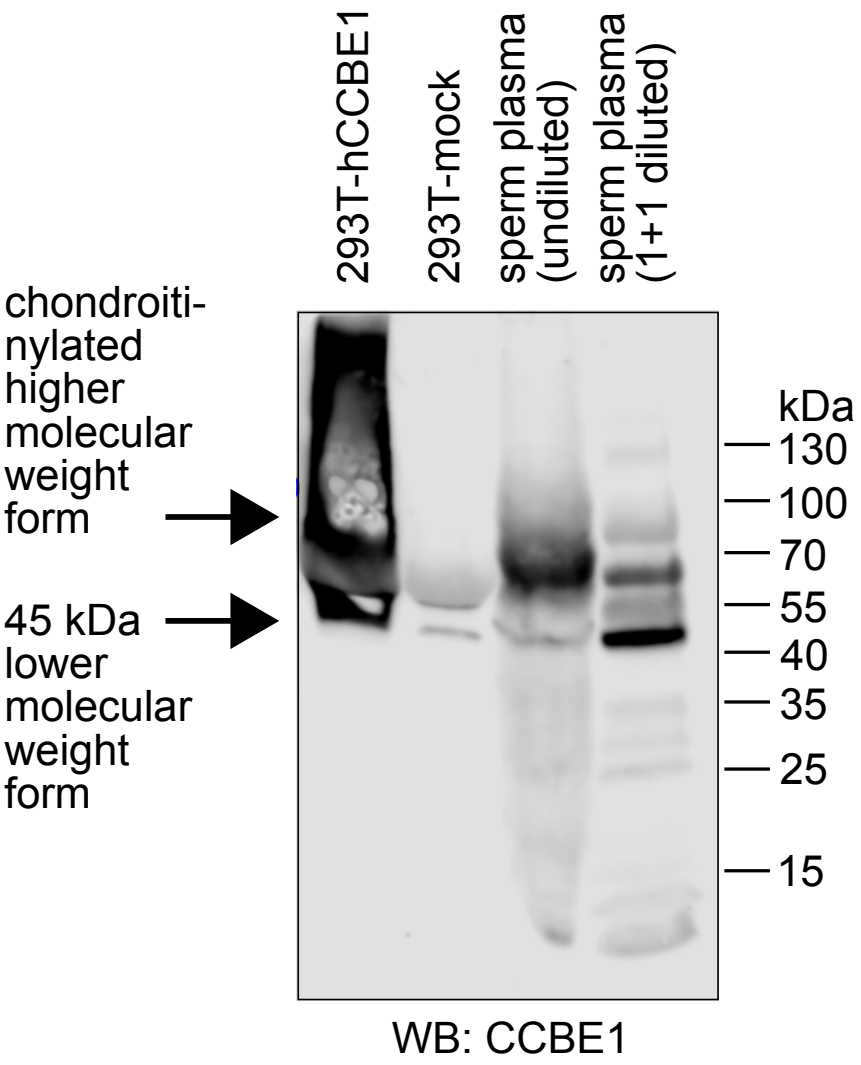

Figure 4-figure supplement 1. Seminal plasma contains CCBE1 protein

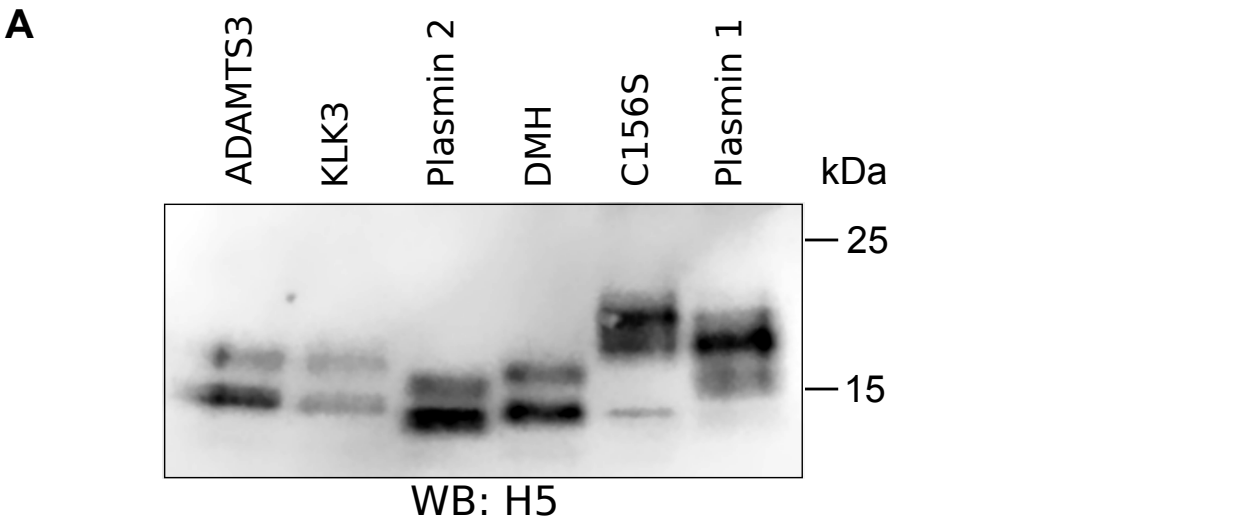

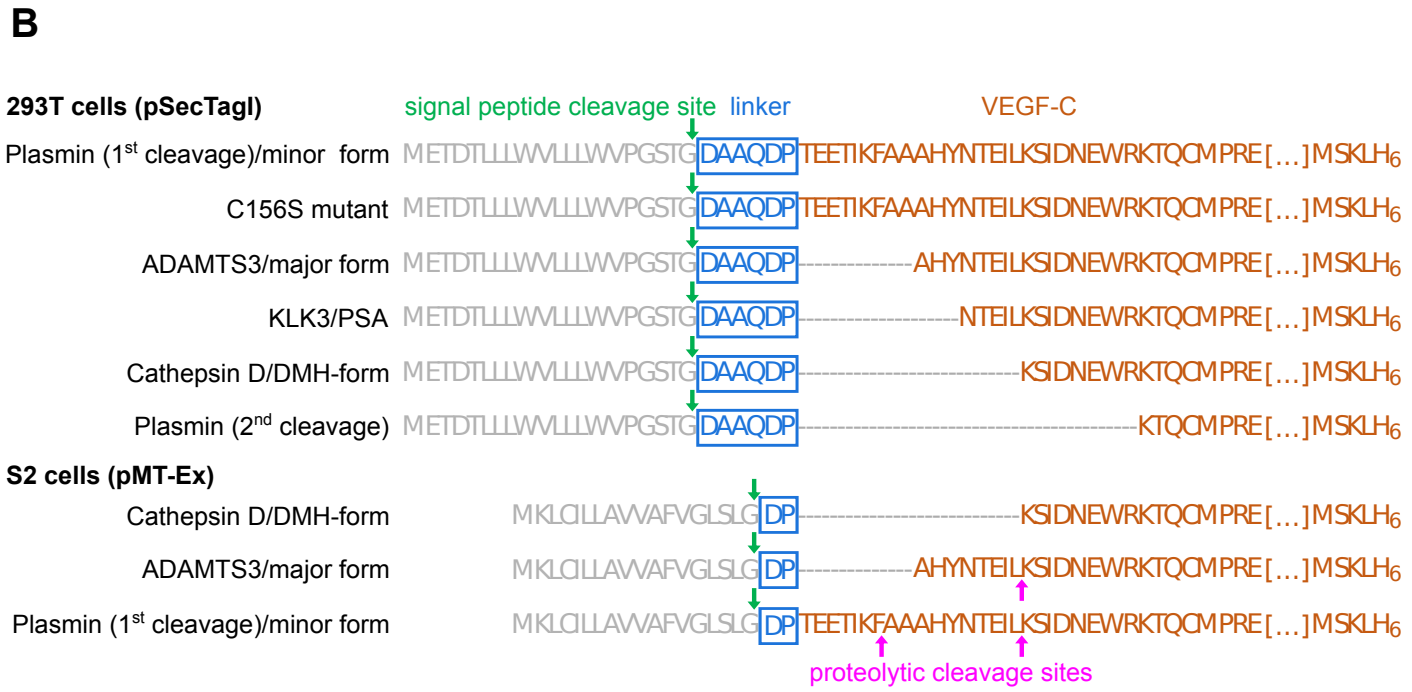

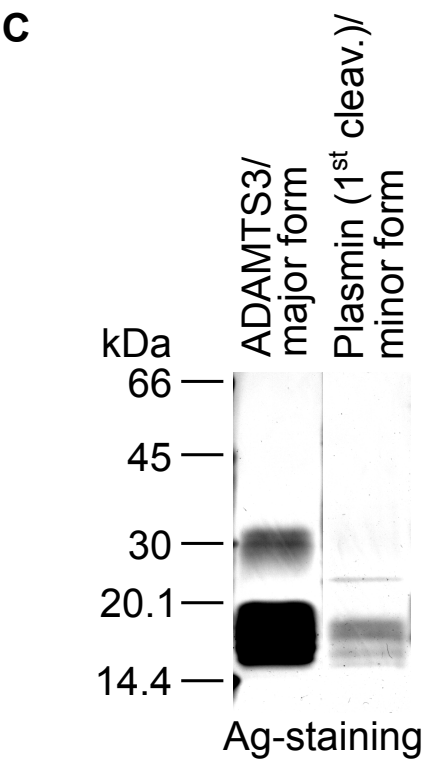

Figure 5-figure supplement 1. Secondary activation of the longer mature VEGF-C form in S2 cells

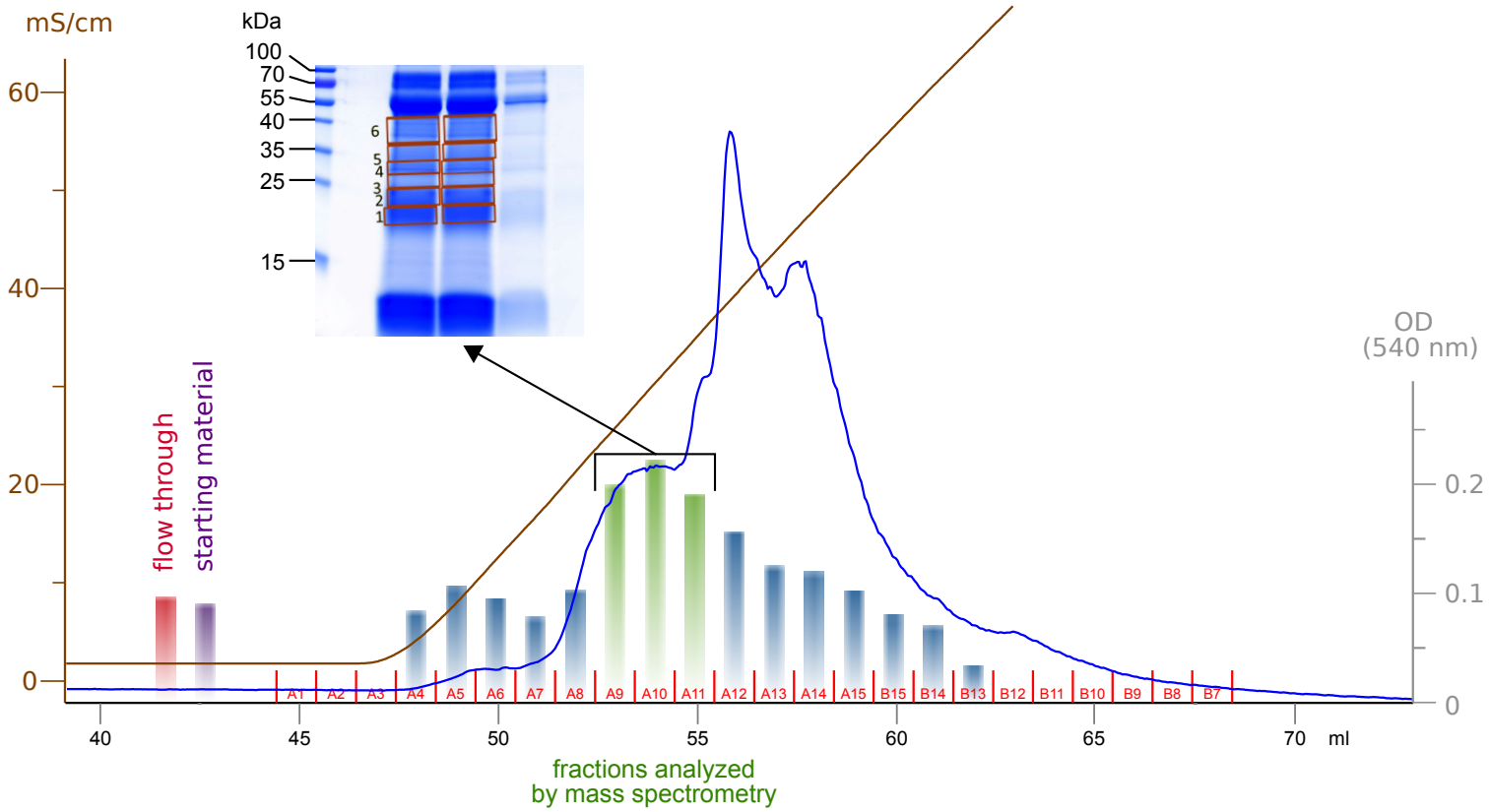

Figure 6-figure supplement 1. Enrichment and fractionation of VEGF-C cleaving activity

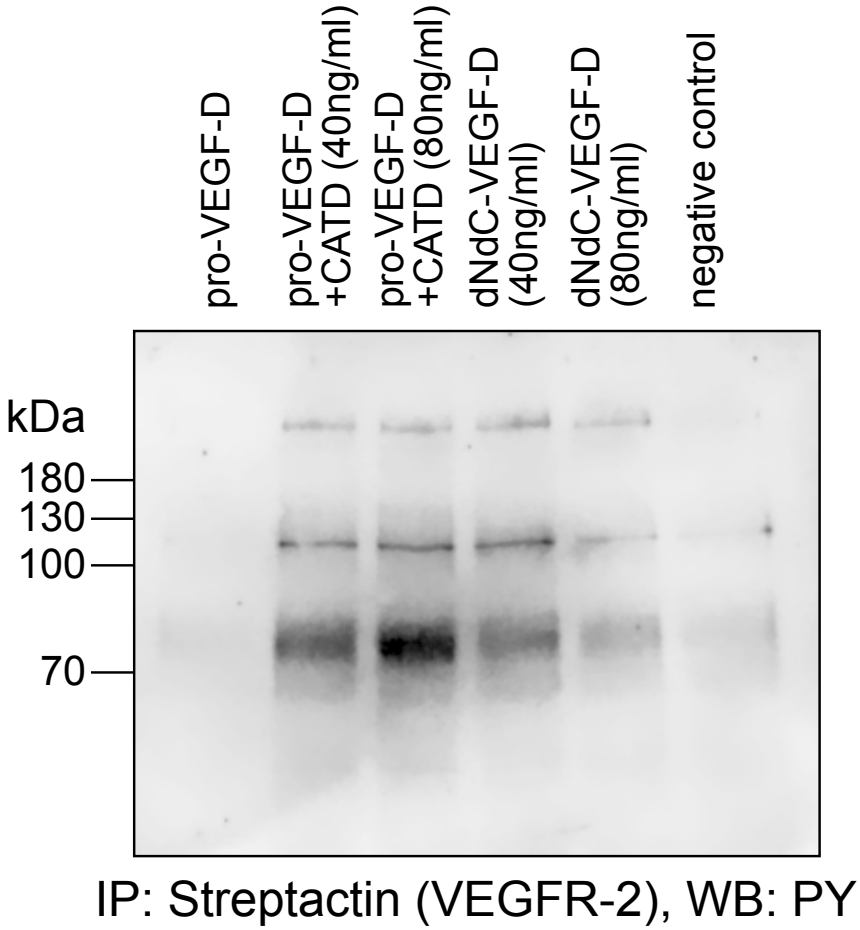

Figure 7-figure supplement 1. Cathepsin D-cleaved pro-VEGF-D stimulates the phosphorylation of VEGFR-2 in PAE cells

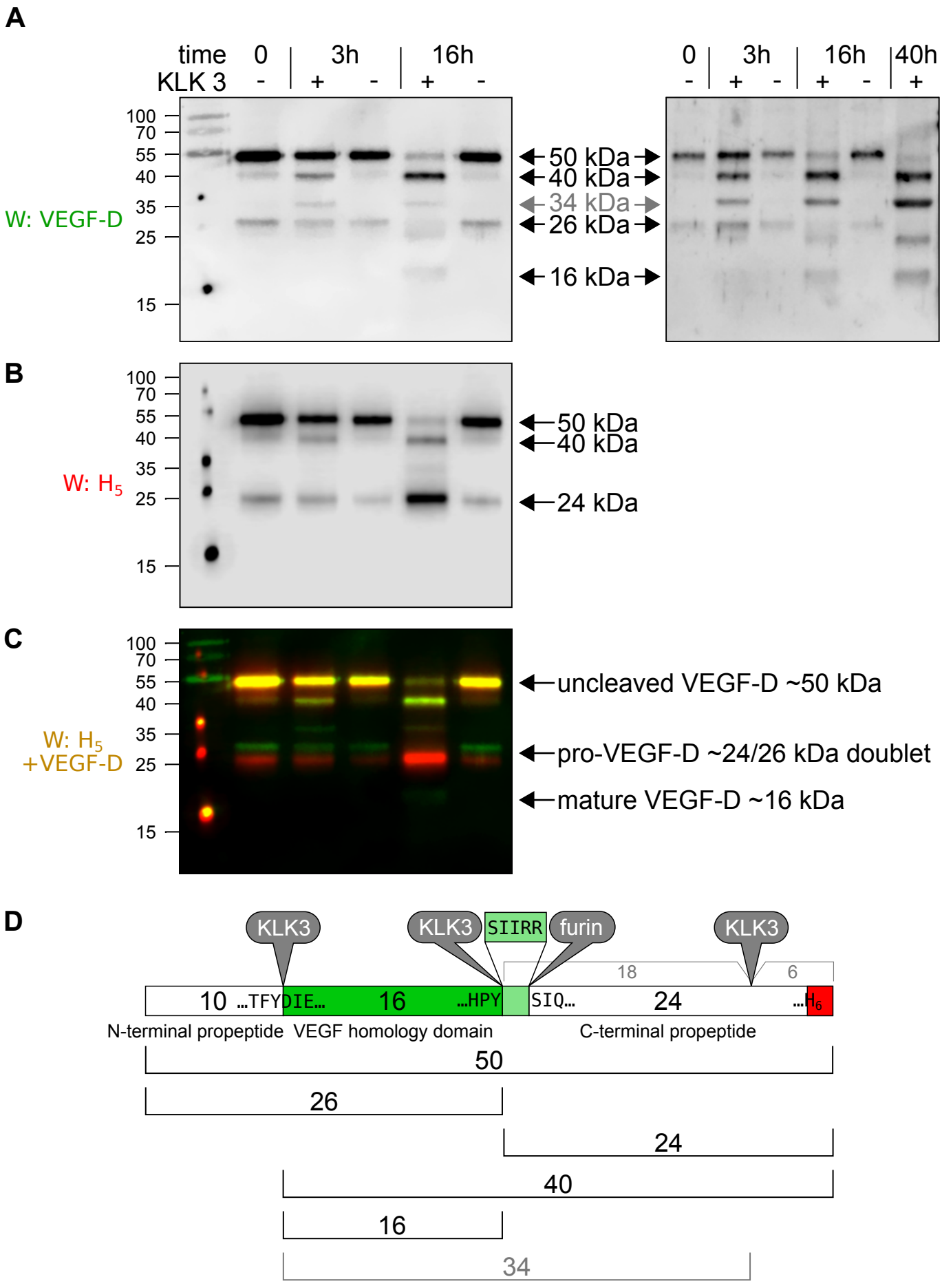

Figure 7-figure supplement 2: KLK3/PSA can proteolytically remove both propeptides from VEGF-D

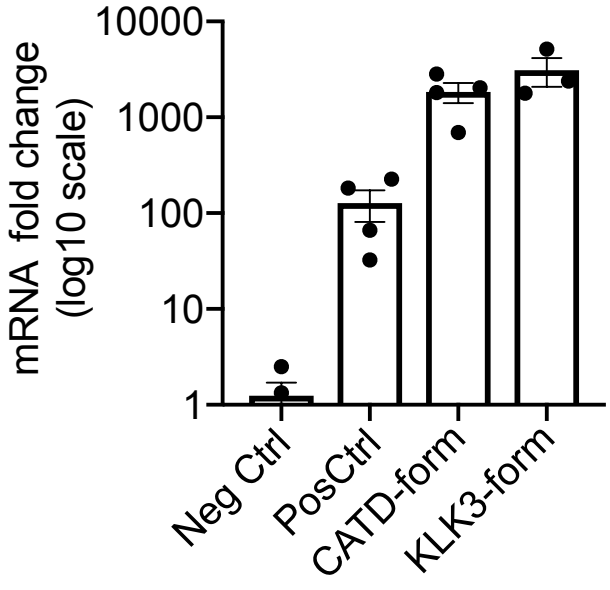

Figure 8-figure supplement 1: Expression of VEGF-C mRNA in tibialis anterior (TA) muscle